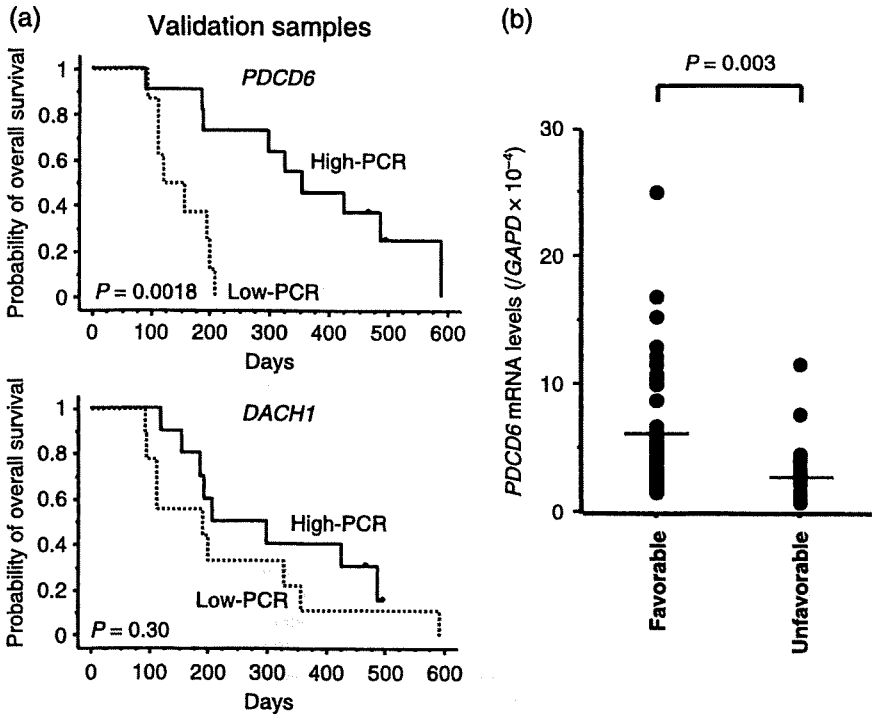

Fig. 3. Results of real-time reverse transcription polymerase chain reaction (RT-PCR) analysis and patient survival in the independent validation set of 19 samples. (a) The Kaplan–Meier method was used to estimate the overall survival. The low *PDCD6* expression groups had significantly poorer outcomes ($P = 0.0018$). High-PCR, group with high expression levels as determined by PCR. Low-PCR, group with low expression levels as determined by PCR. (b) All quantified expression levels of real time RT-PCR data are shown. The mRNA expressions of *PDCD6* were significantly lower in unfavorable group ($P = 0.003$) and varied ~25 fold (range, 0.98–25.1). Favorable, the patients with survival time over 180 days. Unfavorable, the patients with a survival time less than 180 days.

Table 3. Multivariate analysis of prognosis-related genes

Variable	Hazard ratio	95% confidence interval	*P*-value
Age (≥65)	1.78	0.570–5.559	0.3212
Sex (male)	3.26	0.732–14.489	0.1210
Performance status (≥1)	2.36	0.687–8.078	0.1728
Metastasis (≥3)	1.58	0.450–5.561	0.4739
Chemotherapy (5-FU)	1.48	0.402–5.475	0.5541
DACH1	0.38	0.175–0.817	0.0134
EGFR	1.41	0.992–2.001	0.0553
MT1X	0.71	0.317–1.600	0.4111
YWHAE	1.91	0.401–9.061	0.4169
GPX3	1.62	0.869–3.007	0.1293
PDCD6	0.06	0.010–0.334	0.0015
WDR33	1.38	0.268–7.067	0.7017
C14orf43	0.64	0.122–3.407	0.6045
MYLIP	0.67	0.221–2.042	0.4826
GKAP1	2.31	0.751–7.106	0.1440

Cox regression model was performed for multivariate analysis against each of the variables.

Table 4. Results of real-time *RT-PCR* for *PDCD6* and *DACH1* in an independent valiation set

Genes	Hazard ratio	95% confidence limits		*P*-value
		Upper	Lower	
*PDCD6**	0.29	0.12	0.71	0.007
DACH1	0.79	0.56	1.13	0.199

*, $P < 0.05$.

the uncontrollable factors, we aimed to avoid controllable factors with our best efforts. In this sense, we believe that the present study has succeeded in stratifying potential controllable variables.

Based on the results of the series of analyses conducted in the current study, we validated *PDCD6* as a molecular biomarker of the prognosis in gastric cancer.

PDCD6, also known as ALG-2 (apoptosis-linked gene-2), was first identified in a study on T-cell apoptosis conducted by Vito *et al.*[29] *PDCD6* encodes a calcium-binding protein that belongs to the penta-EF-hand protein family. The gene product participates in T-cell receptor-, Fas- and glucocorticoid-induced programmed cell death and cell proliferation. The stimulation of cells to enter the cell cycle is thought to drive the cellular apoptotic program, and the presence of additional survival or pro-apototic signals determines whether a cell proliferates or commits suicide. Krebs *et al.* indicated that the deregulation of such an obviously delicate balance could lead to pathological developments, such as cancer.[30] Detailed biological function of *PDCD6* genes in gastric cancer is still unclear. The speculated function may lead us to hypothesize that the expression is generally downregulated in cancer.

Our ultimate goal is to use real-time RT-PCR or immunohistochemical examination to identify patients with a poor prognosis prior to undertaking chemotherapy. We are now planning a large-scale prospective study based on the evidence obtained in the current study.

In conclusion, we identified prognostic biomarkers in patients with unresected gastric cancer, and our PCR-based single gene prediction strategy successfully predicted the overall survival of patients with gastric cancer. Our findings may provide a novel insight into the treatment of gastric cancer and may lead to a better understanding of this disease subgroup.

Acknowledgments

This work was supported by funds for the Third Term Comprehensive 10-Year Strategy for Cancer Control, a Grant-in-Aid for Scientific Research and the program for promotion of Fundamental Studies in Health Sciences of the National Institute of Biomedical Innovation (NiBio). The following people have played very important roles in the conduct of this project: Hiromi Orita, Hisanao Hamanaka, Ayumu Goto, Hisateru Yasui, Junichi Matsubara, Natsuko Okita, Takako Nakajima,

doi: 10.1111/j.1349-7006.2008.00935.x

Atsuo Takashima, Kei Muro, Takashi Ura, Hideko Morita, Mari Araake, Hisao Fukumoto, Tatsu Shimoyama, Naoki Hayama, Masayuki Takeda, Hideharu Kimura, Kazuko Sakai, Terufumi Kato and Jun-ya Fukai. We also thank Dr Richard Simon and Dr Amy Peng for providing us with the BRB ArrayTools software. This free software was very useful and has been developed for user-friendly applications.

References

1 Sastre J, Garcia-Saenz JA, Diaz-Rubio E. Chemotherapy for gastric cancer. *World J Gastroenterol* 2006; **12**: 204–13.
2 Vanhoefer U, Rougier P, Wilke H *et al.* Final results of a randomized phase III trial of sequential high-dose methotrexate, fluorouracil, and doxorubicin versus etoposide, leucovorin, and fluorouracil versus infusional fluorouracil and cisplatin in advanced gastric cancer: a trial of the European Organization for Research and Treatment of Cancer Gastrointestinal Tract Cancer Cooperative Group. *J Clin Oncol* 2000; **18**: 2648–57.
3 Ohtsu A, Shimada Y, Shirao K *et al.* Randomized phase III trial of fluorouracil alone versus fluorouracil plus cisplatin versus uracil and tegafur plus mitomycin in patients with unresectable, advanced gastric cancer: The Japan Clinical Oncology Group Study (JCOG9205). *J Clin Oncol* 2003; **21**: 54–9.
4 Sakata Y, Ohtsu A, Horikoshi N, Sugimachi K, Mitachi Y, Taguchi T. Late phase II study of novel oral fluoropyrimidine anticancer drug S-1 (1M tegafur-0.4M gimestat-1M otastat potassium) in advanced gastric cancer patients. *Eur J Cancer* 1998; **34**: 1775–20.
5 Koizumi W, Kurihara M, Nakano S, Hasegawa K. Phase II study of S-1, a novel derivative of 5-fluorouracil, in advanced gastric cancer. *Oncology* 2000; **58**: 191–7.
6 Shirao K, Shimada Y, Kondo H *et al.* Phase I–II study of irinotecan hydrochloride combined with cisplatin in patients with advanced gastric cancer. *J Clin Oncol* 1997; **15**: 921–7.
7 Boku N, Ohtsu A, Shimada Y *et al.* Phase II study of combination of irinotecan and cisplatin against metastatic gastric cancer. *J Clin Oncol* 1999; **17**: 319–23.
8 Boku N, Yamamoto S, Shirao K *et al.* Gastrointestinal Oncology Study Group/Japan Clinical Oncology Group. Randomized phase III study of 5-fluorouracil (5-FU) alone versus combination of irinotecan and cisplatin (CP) versus S-1 alone in advanced gastric cancer (JCOG9912) (Abstract). *Proc Am Soc Clin Oncol* 2007; **25**: 18S.
9 Chau I, Norman AR, Cunningham D, Waters JS, Oates J, Ross PJ. Multivariate prognostic factor analysis in locally advanced and metastatic esophago-gastric cancer – pooled analysis from three multicenter, randomized, controlled trials using individual patient data. *J Clin Oncol* 2004; **22**: 2395–403.
10 Metzger R, Leichman CG, Danenberg KD *et al.* ERCC1 mRNA levels complement thymidylate synthase mRNA levels in predicting response and survival for gastric cancer patients receiving combination cisplatin and 5-fluorouracil chemotherapy. *J Clin Oncol* 1998; **16**: 309–16.
11 Boku N, Chin K, Hosokawa K *et al.* Biological makers as a predictor for response and prognosis of unresectable gastric cancer patients treated with 5-fluorouracil and cis-platinum. *Clin Cancer Res* 1998; **4**: 1469–74.
12 Yonemura Y, Ninomiya I, Yamaguchi A *et al.* Evaluation of immunoreactivity for erbB-2 protein as a marker of poor short term prognosis in gastric cancer. *Cancer Res* 1991; **51**: 1034–8.
13 Sanz-Ortega J, Steinberg SM, Moro E *et al.* Comparative study of tumor angiogenesis and immunohistochemistry for p53, c-ErbB2, c-myc and EGFr as prognostic factors in gastric cancer. *Histol Histopathol* 2000; **15**: 455–62.
14 Shibata A, Parsonnet J, Longacre TA *et al.* CagA status of *Helicobacter pylori* infection and p53 gene mutations in gastric adenocarcinoma. *Carcinogenesis* 2002; **23**: 419–24.
15 Okusa Y, Ichikura T, Mochizuki H. Prognostic impact of stromal cell-derived urokinase-type plasminogen activator in gastric carcinoma. *Cancer* 1999; **85**: 1033–8.
16 Linder N, Haglund C, Lundin M *et al.* Decreased xanthine oxidoreductase is a predictor of poor prognosis in early-stage gastric cancer. *J Clin Pathol* 2006; **59**: 965–71.
17 Resnick MB, Gavilanez M, Newton E *et al.* Claudin expression in gastric adenocarcinomas: a tissue microarray study with prognostic correlation. *Hum Pathol* 2005; **36**: 886–92.
18 Kido S, Kitadai Y, Hattori N *et al.* Interleukin 8 and vascular endothelial growth factor – prognostic factors in human gastric carcinomas? *Eur J Cancer* 2001; **37**: 1482–7.
19 Xiangming C, Natsugoe S, Takao S *et al.* The cooperative role of p27 with cyclin E in the prognosis of advanced gastric carcinoma. *Cancer* 2000; **89**: 1214–9.
20 Yasui W, Oue N, Ono S, Mitani Y, Ito R, Nakayama H. Histone acetylation and gastrointestinal carcinogenesis. *Ann NY Acad Sci* 2003; **983**: 220–31.
21 Oue N, Motoshita J, Yokozaki H *et al.* Distinct promoter hypermethylation of p16INK4a, CDH1, and RAR-beta in intestinal, diffuse-adherent, and diffuse-scattered type gastric carcinomas. *J Pathol* 2002; **198**: 55–9.
22 Yamanaka R, Arao T, Yajima N *et al.* Identification of expressed genes characterizing long-term survival in malignant glioma patients. *Oncogene* 2006; **25**: 5994–6002.
23 Hasegawa S, Furukawa Y, Li M *et al.* Genome-wide analysis of gene expression in intestinal-type gastric cancers using a complementary DNA microarray representing 23 040 genes. *Cancer Res* 2002; **62**: 7012–17.
24 Hippo Y, Taniguchi H, Tsutsumi S *et al.* Global gene expression analysis of gastric cancer by oligonucleotide microarrays. *Cancer Res* 2002; **62**: 233–40.
25 Inoue H, Matsuyama A, Mimori K, Ueo H, Mori M. Prognostic score of gastric cancer determined by cDNA microarray. *Clin Cancer Res* 2002; **8**: 3475–9.
26 Leung SY, Yuen ST, Chu KM *et al.* Expression profiling identifies chemokine (C-C motif) ligand 18 as an independent prognostic indicator in gastric cancer. *Gastroenterology* 2004; **127**: 457–69.
27 Leung SY, Chen X, Chu KM *et al.* Phospholipase A2 group IIA expression in gastric adenocarcinoma is associated with prolonged survival and less frequent metastasis. *Proc Natl Acad Sci USA* 2002; **99**: 16203–8.
28 Chen CN, Lin JJ, Chen JJ *et al.* Gene expression profile predicts patient survival of gastric cancer after surgical resection. *J Clin Oncol* 2005; **23**: 7286–95.
29 Vito P, Lacana E, D'Adamio L. Interfering with apoptosis: $Ca^{(2+)}$-binding protein ALG-2 and Alzheimer's disease gene ALG-3. *Science* 1996; **271**: 521–5.
30 Krebs J, Saremaslani P, Caduff R. ALG-2: a Ca^{2+}-binding modulator protein involved in cell proliferation and in cell death. *Biochim Biophys Acta* 2002; **1600**: 68–73.

Antitumor activity of cetuximab against malignant glioma cells overexpressing EGFR deletion mutant variant III

Junya Fukai,[1,2] Kazuto Nishio,[3] Toru Itakura[2] and Fumiaki Koizumi[1,4]

[1]Shien-Laboratory, National Cancer Center Hospital, Tsukiji 5-1-1, Chuo-ku, Tokyo, 104-0045; [2]Department of Neurological Surgery, Wakayama Medical University, Kimiidera 811-1, Wakayama, 641-0012; [3]Department of Genome Biology, Kinki University School of Medicine, Ohno-higashi 377-2, Osaka-sayama, Osaka, 589-8511, Japan

(Received February 22, 2008/Revised June 17, 2008/Accepted June 19, 2008/Online publication October 3, 2008)

Anti-epidermal growth factor receptor (EGFR) monoclonal antibody, cetuximab, is a promising targeted drug for EGFR-expressing tumors. Glioblastomas frequently overexpress EGFR including not only the wild type but also a deletion mutant form called 'variant III (vIII)', which lacks exon 2–7, does not bind to ligands, and is constitutively activated. In this study, we investigated the antitumor activity of cetuximab against malignant glioma cells overexpressing EGFRvIII. For this purpose, we transfected human malignant glioma cell lines with the retroviral vector containing cDNA for EGFRvIII, and analyzed the mode of cetuximab-induced action on the EGFRvIII in the cells. Immunoprecipitation and immunofluorescence revealed binding of cetuximab to EGFRvIII. Notably, immunoblotting analyses showed that cetuximab treatment resulted in reduced expression levels of the EGFRvIII. However, cetuximab alone did not exhibit a growth-inhibitory effect against the EGFRvIII-expressing cells. On the other hand, an assay for antibody-dependent cell-mediated cytotoxicity (ADCC) demonstrated cetuximab-induced cytolysis in the presence of human peripheral blood mononuclear cells in a dose-dependent manner. These results suggest that deletion mutant EGFRvIII can be a target of cetuximab and that ADCC activity substantially contributes to the antitumor efficacy of cetuximab against the EGFRvIII-expressing glioma cells. Thus, cetuximab could be a promising therapy in malignant gliomas that express EGFRvIII. (*Cancer Sci* 2008; 99: 2062–2069)

Long-term survival of patients with malignant gliomas has not substantially improved despite aggressive multimodality treatments including cytoreductive surgery, radiotherapy, and cytotoxic chemotherapy. To efficiently suppress these tumors, additional therapeutic strategies are necessary. Understanding the molecular genetics, biology, and immunology of gliomas will enable the potential development of new adjuvant treatments for malignant glioma patients.

Malignant gliomas may arise via a heterogeneous process resulting from multiple genetic alterations.[1] One of the well-known molecular features of gliomas is amplification of the epidermal growth factor receptor (*EGFR*) gene, leading to overexpression of this receptor in approximately 40–60% of glioblastomas.[2,3] High levels of EGFR expression have been shown to be correlated with malignant progression in gliomas and associated with a poor prognosis and resistance to therapies.[4] Therefore, therapeutic strategies directed against the EGFR may have potential in these malignancies.

In the EGFR-amplified tumors, multiple types of EGFR mutations can be detected as a result of intragene deletions.[2] The most frequent mutation in malignant gliomas is EGFR variant III (EGFRvIII), characterized by a consistent and tumor-specific in-frame deletion of 801 base pairs from the coding sequence of the extracellular domain.[5,6] This mutated gene encodes a protein with a ligand-independent and constitutively active tyrosine kinase domain, which greatly enhances the tumorigenicity of the cells, mostly found *in vivo*, not *in vitro*.[7–9] The deletion mutant EGFRvIII, which is clonally expressed on the cell surface of ~40% of glioblastomas, has been clinically correlated with increased glioma cell growth, proliferation, invasion, and angiogenesis.[2,10,11] For the EGFR-targeted strategies in malignant glioma therapy, EGFRvIII expression should be considered because of its highly malignant nature.

Methods of targeting the EGFR that have been developed and trialed include monoclonal antibodies (mAbs), synthetic tyrosine kinase inhibitors, conjugates of toxins to anti-EGFR mAbs and ligands, and antisense gene therapy of EGFR.[12,13] Small molecule tyrosine kinase inhibitors and mAbs are the most fully developed of these approaches.[14,15]

Cetuximab (Erbitux, IMC-C225) is a recombinant, human-murine chimeric mAb specifically targeting the EGFR.[13] Cetuximab competes with endogenous ligands for binding to the extracelluar domain of EGFR and binding of cetuximab prevents stimulation of the receptor by ligands. Cetuximab-binding also results in internalization of the antibody-receptor complex which leads to down-regulation of EGFR expression on the cell surface.[13] Furthermore, this type of mAb including the human IgG1 Fc region may cause recruitment and activation of host immune-effector cells (T cells, natural-killer cells, and macrophages) or complements to induce antibody-dependent cell-mediated cytotoxicity (ADCC) or complement-dependent cytotoxicity (CDC).[16,17]

A variety of human epithelial cancers expressing EGFR have been successfully treated by cetuximab with promising results and it was recently approved for use in treating advanced-stage EGFR-expressing colorectal, head, and neck cancers.[13,18] However, little is known as to whether or not it is an effective therapy for the treatment of highly malignant tumors expressing deletion mutant EGFRvIII. Based on the encouraging results of cetuximab in the EGFR-expressing cancers and the importance of EGFRvIII expression in the biology of glioblastomas, we investigated whether cetuximab would be capable of effectively targeting the EGFRvIII expressed in malignant glioma cell lines.

Materials and Methods

Cell culture. Human glioblastoma cell lines were obtained as follows: U-251 MG, A-172, SF126, and YH-13, JCRB Cell Bank (Osaka, Japan); U-118 MG, U-87 MG, DBTRG-05 MG, LN-229,

[4]To whom correspondence should be addressed.
E-mail: fkoizumi@gan2.res.ncc.go.jp

doi: 10.1111/j.1349-7006.2008.00945.x

LN-18, and M059K, ATCC (Manassas, VA, USA). These cell lines were maintained in RPMI-1640 supplemented with 10% fetal bovine serum and cultured at 37°C in a humidified atmosphere containing 5% CO_2.

Expression vector construction and cell transfection. Construction of expression vector was generously contributed by Dr Hideyuki Yokote (Wakayama, Japan). Full-length cDNA of wild-type (wt) EGFR was amplified by reverse transcription–polymerase chain reaction (RT-PCR) from a human embryonal kidney cell line HEK293 using a High Fidelity RNA PCR Kit (TaKaRa, Shiga, Japan) and the following primer sets: forward, CGCTAGCGATGCGACCCTCCGGGAC; reverse, CCCCTGACTCCGTCCAGTATTGA. The PCR products were amplified using the following primer sets: forward, CGCTAGCGATGCGACCCTCCGGGAC; reverse, CGAAGCTTTGCTCCAATAAATTCACTGC. The amplified DNA included NheI- and HindIII-cut cohesive ends at the 5′- and 3′-ends, respectively. The product was subcloned into a pCR BluntII-TOPO vector (Invitrogen, Carlsbad, CA, USA) and the sequences were confirmed. Oligonucleotides encoding the myc-tag sequence (EQKLISEEDLN) were designed and synthesized as follows: forward, AGCTTGAACAGAAGCTGATCTCAGAGGAGGACCTGAATTGAC; reverse, TCGAGTCAATTCAGGTCCTCCTCTGAGATCAGCTTCTGTTCA. These oligos were annealed, and the ds-oligos were generated including HindIII- and XhoI-cut cohesive ends, at the 5′- and 3′-ends, respectively. Wt EGFR and myc-tag DNA fragments were cut out and transferred into a pQCXIX retroviral vector (BD Biosciences Clontech, San Diego, CA, USA) containing EGFP following internal ribosome entry site sequence. EGFRvIII was synthesized with the recombinant PCR method using the following primers: F1, CGCTAGCGATGCGACCCTCCGGGAC; R1, ATCTGTCACCACATAATTACCTTTCTTTTCCTCCAGAGCC; F2, GGCTCTGGAGGAAAAGAAAGGTAATTATGTGGTGACAGAT; R2, CGGTGGAGGTGAGGCAGATG. Two DNA fragments of wt EGFR were amplified using the F1/R1 and F2/R2 primer sets. The EGFR fragment deleting exon 2–7 was amplified using the two PCR products as templates and the F1/R2 primer set. After confirming the sequence, a wt EGFR fragment was substituted for the NheI- and EcoRI- cut recombinant PCR fragment. A pVSV-G vector (BD Biosciences Clontech) and the pQCXIX constructs were cotransfected into the GP2-293 cells (BD Biosciences Clontech) using a FuGENE6 transfection reagent (Roche Diagnostics, Basel, Switzerland). Briefly, 80% confluent cells cultured on a 10-cm dish were transfected with 2-mg pVSV-G plus 6-mg pQCXIX vectors. Forty-eight h after transfection, culture medium was collected and the viral particles were concentrated by centrifugation. The viral pellet was resuspended in fresh medium. The titer of the viral vector was calculated by counting the EGFP-positive cells which were infected by serial dilution of the virus-containing medium and the multiplicity of infection was determined.

Chemicals. Cetuximab was kindly provided by Brystol-Myers Squibb (Princeton, NJ, USA).

Antibodies. Abs were purchased as follows: antihuman EGFR mouse mAb cocktail, Biosource Corp. (Camarillo, CA, USA); antiphosphotyrosine mouse mAb, BD Biosciences; antiphospho-Akt, phospho-p44/42 mitogen activated protein kinase (MAPK), rabbit polyclonal, anti-β-actin rabbit monoclonal, and antimouse and rabbit IgG horseradish peroxidase–linked Abs, Cell Signaling Technology (Beverly, MA, USA).

Immunoblotting. Cells were seeded and grown to near confluency. Then, cells were washed with phosphate-buffered saline (PBS) and culture medium with or without cetuximab was added. At the time of harvest, cells were washed and lyzed with lysis buffer (50 mM Hepes buffer, 1% Triton X-100, 5 mM ethylenediaminetetraacetic acid [EDTA], 50 mM sodium chloride, 10 mM sodium pyrophosphate, 50 mM sodium fluoride, and 1 mM sodium orthovanadate) supplemented with protease inhibitors (Roche Diagnostics, Penzberg, Germany). Cell lysates were clarified by centrifugation, and equal concentrations of lysates were mixed with 4× sodium dodecyl sulfate (SDS)–gel sample buffer (0.25 mol/L Tris-HCl, pH 6.8, 2% SDS, and 25% glycerol), denatured with 2-mercaptoethanol. Equivalent amounts of protein were separated on SDS-polyacrylamide gels by electrophoresis, and transferred onto polyvinylidene difluoride (PVDF) membranes by wet electroblotting. The PVDF membranes were blocked with 3% bovine serum albumin in PBS with 0.1% Tween-20 and probed with primary Ab. The membranes were washed and incubated with secondary Ab. After the membranes were washed, immunoblotted proteins were detected using the ECL Western Blotting Detection System (GE Healthcare, Buckinghamshire, UK).

Immunoprecipitation. Cell lysates were extracted and treated with Ab overnight at 4°C. The lysates were mixed with protein A agarose and centrifuged. Immunoprecipitates were washed with lysis buffer and resuspended in 1.5× SDS-sample buffer and denatured with 2-mercaptoethanol. Samples were processed by immunoblotting.

Immunofluorescence. For immunofluorescence, cells were grown overnight, washed in PBS and fixed for 20 min in 4% paraformaldehyde at room temperature (RT). Cells were then washed twice in PBS and blocked for 1 h in 10% normal goat serum at RT. Cetuximab (10 mg/mL) was diluted in 1.5% normal goat serum and incubated overnight at 4°C. Cells were washed twice in PBS for 5 min and incubated with a secondary Ab for 45 min at RT. Secondary Abs included Alexa Fluor 546 Goat Anti-Mouse IgG (2 mg/mL; Molecular Probes, Invitrogen) and Texas Red antihuman IgG (1.5 mg/mL; Vector, Burlingame, CA, USA). Cells were washed twice for 5 min in PBS and then examined under a microscope (Keyence Biozero, Osaka, Japan).

Growth-inhibition assay (MTS assay). The growth-inhibitory effect of cetuximab was evaluated using the CellTiter96 Aqueous One Solution Cell Proliferation Assay (Promega Corporation, Madison, WI, USA). MTS (3-[4,5-dimethylthiazol-2-yl]-5-[3-carboxymethoxyphenyl]-2-[4-sulfophenyl]-2H-tetrazolium, inner salt) provides a measure of mitochondrial dehydrogenase activity within the cell and thereby offers an indication of cellular proliferation status.[19] Briefly, 3000 cells were seeded in 96-well plates. The plates were incubated overnight to permit adherence. Cells were then exposed to different concentrations of cetuximab ranging from 0 to 100 mg/mL for 48 h. MTS reagent was added and incubated for 1 h. The plates were read on a microplate spectrophotometer (optical density, 490 nm). The percentage cell growth was calculated by comparison of the absorbance value reading obtained from treated samples *versus* controls.

Antibody-dependent cell-mediated cytotoxicity (ADCC). Peripheral blood mononuclear cells (PBMCs) were separated from whole blood of healthy volunteers using LSM Lymphocyte Separation Medium (Cappel, Aurora, OH, USA). 1×10^5 cells were seeded into each well of a 12-well plate. After incubation for 24 h, human PBMCs alone (effector : target = 10:1), and/or cetuximab (10 mg/mL), control human IgG (10 mg/mL), or control medium were added to the wells. The cultures were then examined under a microscope (Keyence) 24-h post treatment.

Propidium iodide (PI) nucleic acid stain for cetuximab-mediated ADCC. This assay was performed for identifying dead cells in a population under the same experimental condition as described in the 'ADCC' section. A 4-μM solution of Cellstain PI (1 mg/mL; Dojindo, Kumamoto, Japan) was made at a dilution rate of 1:3000 and added per well. After incubation in the dark for 15 min, cells were viewed under a microscope (Keyence).

MTS assay for cetuximab-mediated ADCC. For analysis of the ADCC activity of cetuximab, we used the MTS assay.[20] Briefly, 3000 cells per well were exposed to various concentrations of cetuximab in the presence of PBMCs at an effector/target (E/T) ratio of 10 for 48 h. Natural killer (NK) activity was calculated from the absorbance value of the cells cultured without cetuximab

and PBMCs (A), the absorbance value of the cells cultured with PBMCs (B), the absorbance value of medium alone (C), and the absorbance value of PBMCs (D) as follows: $\{1 - [(B - C) - (D - C)]/[(A - C) - (D - C)]\} \times 100$. ADCC was calculated from the values of A, D, the NK activity (E), and the absorbance value of the cells treated with cetuximab and PBMCs (F): $\{1 - (F - D)/(A - D)\} \times 100 - E$.

Results

Initially, we determined the expression of endogenous EGFR protein in 10 human malignant glioma cell lines by immunoblotting (Fig. 1a). All of these malignant glioma cell lines displayed only low amounts of wt EGFR protein (170 kDa) but not EGFRvIII protein (145 kDa). These findings were consistent with the previous notion that because primary explants of human glioblastoma rapidly lose expression of amplified, rearranged receptors in culture, no existing glioblastoma cell lines exhibit such expression.[22] Therefore, we introduced the *EGFRvIII* gene into malignant glioma cell lines and engineered them to express this mutant receptor protein in three cell lines: U-251 MG, U-87 MG, and LN-229 (Fig. 1b). Malignant glioma cells that expressed the EGFRvIII protein were observed under fluorescence microscopy due to the coexpression of EGFP (Fig. 1c).

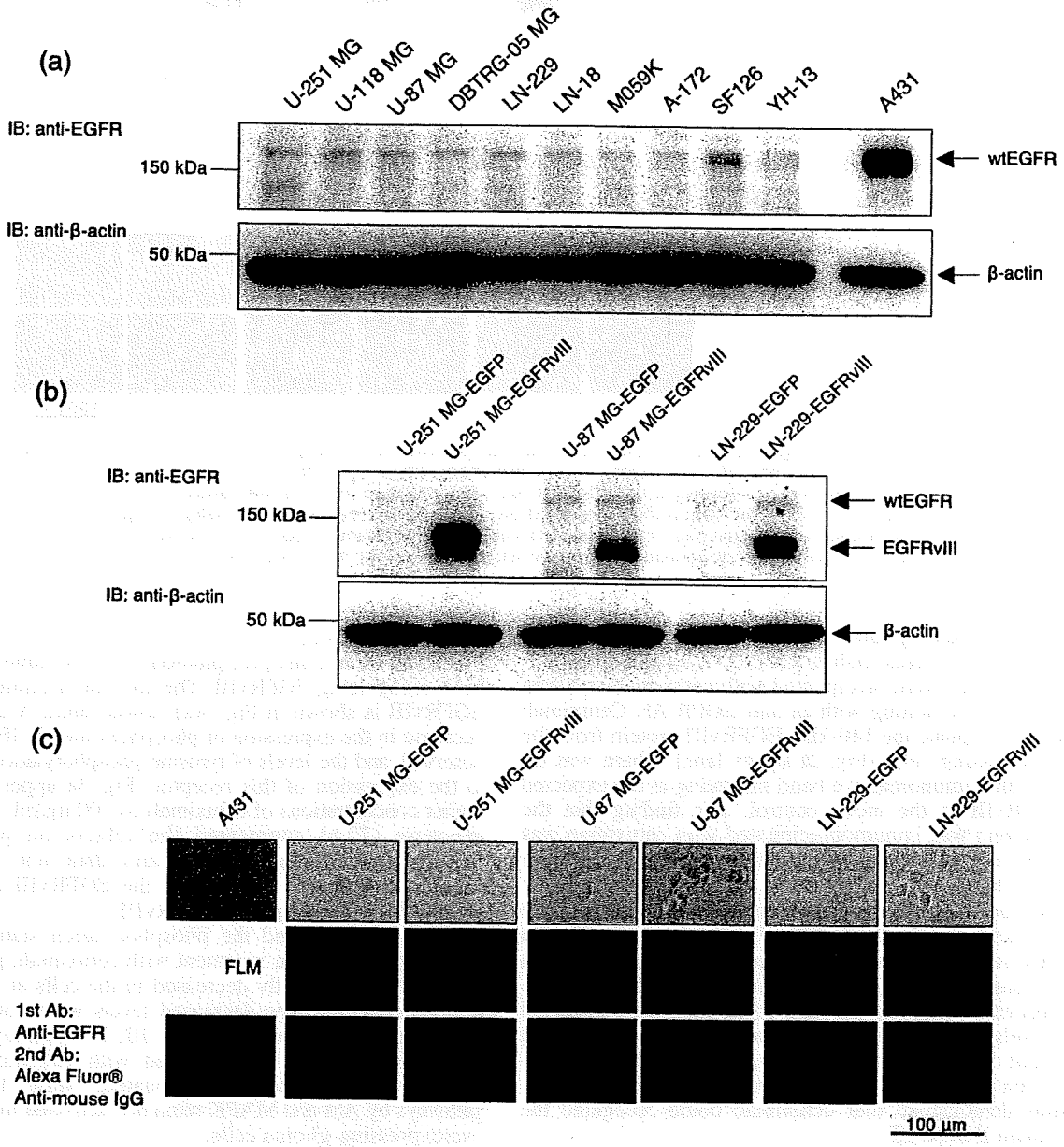

Fig. 1. (a) Expression of epidermal growth factor receptor (EGFR) in human malignant glioma cell lines. Ten malignant glioma cell lines were cultured and lyzed. Equal amounts of cell lysate were immunoblotted with anti-EGFR antibody (Ab) to show endogenous expression of EGFR. The human epidermoid carcinoma A431 cell lines served as a reference marker for high expression of wild-type (wt) EGFR.[21] Beta-actin showed protein loading. IB, immunoblotting. (b) Introduction of EGFRvIII into human malignant glioma cell lines. Three malignant glioma cell lines, into which the *EGFRvIII* gene was introduced, were cultured and lyzed. Equal amounts of cell lysates were immunoblotted with an anti-EGFR Ab to recognize exogenous expression of EGFRvIII. (c) Microscopic images and immunofluorescence of malignant glioma cells expressing EGFRvIII. EGFRvIII-expressing cells (*EGFRvIII*) were monitored by their coexpression of EGFP. Mock control (*EGFP*) expressed only EGFP. FM, fluorescent microscopy. EGFRvIII-expressing cells were stained with anti-EGFR Ab, then Alexa Fluor-conjugated antimouse IgG secondary Ab (lower panels). Staining of A431 or *EGFP* served as a reference of endogeneously expressed wt EGFR. Scale bar represents 100 μm.

doi: 10.1111/j.1349-7006.2008.00945.x

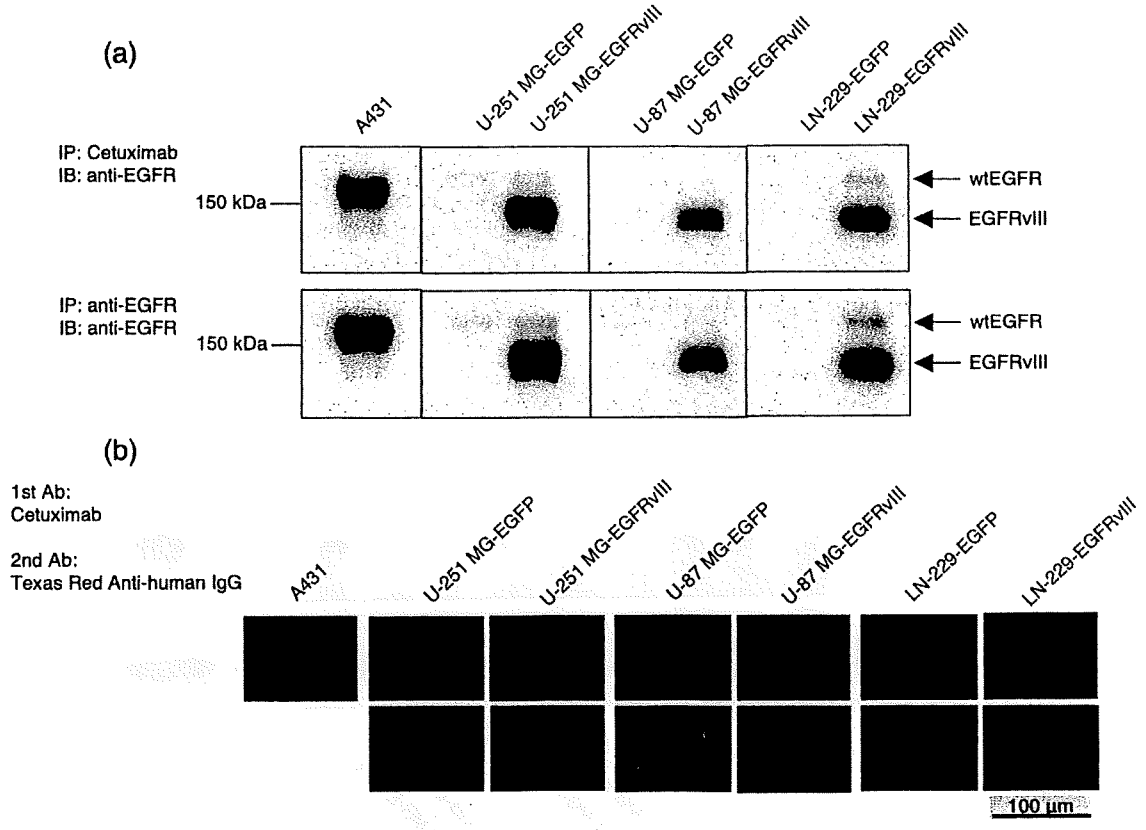

Fig. 2. (a) Immunoprecipitation showing cetuximab binding to epidermal growth factor receptor variant III (EGFRvIII). EGFRvIII-expressing cells were washed and lyzed. Equal amounts of cell lysates were immunoprecipitated with cetuximab or anti-EGFR antibody (Ab). The immunoprecipitates were probed by immunoblotting with anti-EGFR Ab. *A431* was used as a positive control for wild-type (wt) EGFR expression, and *EGFP* as a negative control for EGFRvIII. (b) Immunofluorescence showing cetuximab reactivity with malignant glioma cells expressing EGFRvIII. EGFRvIII-expressing cells were stained with cetuximab, then Texas Red–conjugated antihuman IgG secondary Ab. Staining of A431 or *EGFP* served as a reference for cetuximab reactivity with endogeneously expressed wt EGFR. Scale bar represents 100 μm.

Cetuximab has a binding ability to EGFRvIII. We investigated the binding capability of cetuximab to EGFRvIII by immunoprecipitation. Cell lysates were precipitated with cetuximab and then analyzed by immunoblotting with an anti-EGFR Ab. Cetuximab was found to precipitate the 140-kDa EGFRvIII protein from the EGFRvIII-expressing cells (Fig. 2a upper lane). There was no indication of an immunoreactive band migrating at the expected size of EGFRvIII in the mock control. The finding that the EGFRvIII protein was immunoprecipitated with cetuximab was confirmed by anti-EGFR Ab recognizing this mutant receptor (Fig. 2a lower lane).

Next, we performed immunofluorescence to investigate cetuximab reactivity with the EGFRvIII-overexpressing glioma cells. In this assay, cetuximab was used as a primary Ab, and Texas Red–conjugated antihuman IgG as a secondary Ab. In the mock control expressing low amounts of wt EGFR, we observed very low levels of staining, most of which were close to the detection limit of the analysis (Fig. 2b). In contrast, strong staining was evident in the EGFRvIII-overexpressing cells. Together these results demonstrate that cetuximab could recognize the deletion mutant EGFRvIII.

Cetuximab attenuates EGFRvIII expression and reduces phosphorylated EGFRvIII, but does not significantly inhibit Akt and MAPK signaling pathways. Based on the previous report that cetuximab-binding leads to down-regulation of EGFR expression, we investigated the effect of cetuximab on EGFRvIII expression by immunoblotting.[13] On treatment with cetuximab at various concentrations, the expression levels of EGFRvIII protein decreased dramatically in a dose-dependent manner (data not shown and Fig. 3a lower lane). In addition, we assessed the phosphorylation status of EGFRvIII by immunoprecipitation from the same lysates using a mAb recognizing EGFRvIII. The amount of immunoprecipitated EGFRvIII is shown in Fig. 3(a) (lower lane). A dose-dependent decrease in the expression of phosphorylated EGFRvIII was also observed, and the levels of tyrosine-phosphorylation corresponded to the expression of this receptor (Fig. 3a upper lane). Neither higher concentrations of cetuximab (= 100 μg/mL) nor prolonged exposure (72 h) augmented the effects on phosphorylated EGFRvIII expression (Fig. 3b and data not shown). Thus, cetuximab appeared to attenuate the EGFRvIII expression and reduce the phosphorylated EGFRvIII.

Next, we examined the phosphorylation status of Akt and MAPK pathways. On treatment with cetuximab, phosphorylated Akt and MAPK mildly decreased in the cells at higher concentrations (Fig. 3b). The decreased levels were not so significant as that of phosphorylated EGFRvIII. In summary, these results would suggest that when treated with cetuximab, EGFRvIII expression was markedly attenuated, while its downstream pathways by Akt and MAPK remained activated in the EGFRvIII-overexpressing glioma cells.

Cetuximab does not inhibit the growth of EGFRvIII-overexpressing glioma cells. We examined the effects of cetuximab on the growth of EGFRvIII-overexpressing glioma cells with an MTS assay. As can be observed in Fig. 4, cetuximab treatment did not produce a clear growth-inhibitory effect in the EGFRvIII-overexpressing cells even at the highest concentration tested. Also, treatment with cetuximab had a modest effect on the mock control. These data might support the findings determined by immunoblotting analyses.

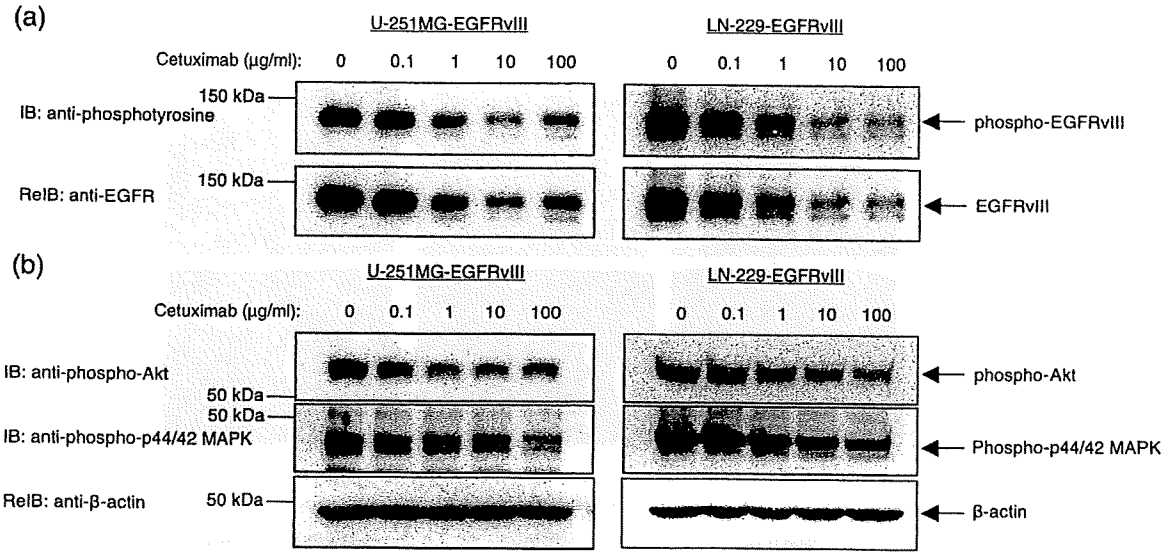

Fig. 3. Effect of cetuximab on epidermal growth factor receptor variant III (EGFRvIII) and its downstream signaling molecules. EGFRvIII-expressing glioma cells were exposed to 0, 0.1, 1, 10, or 100 μg/mL cetuximab for 24 h. (a) 250 μg of total cell lysates were immunoprecipitated with an anti-EGFR antibody (Ab). The immunoprecipitates were probed by immunoblotting with an antiphosphotyrosine Ab (upper lane) and the membranes were reblotted with an anti-EGFR antibody (lower lane). (b) Equal amounts of cell lysates were immunoblotted with a specific antihuman antibody as the first antibody, and then with a horseradish peroxidase–conjugated secondary antibody.

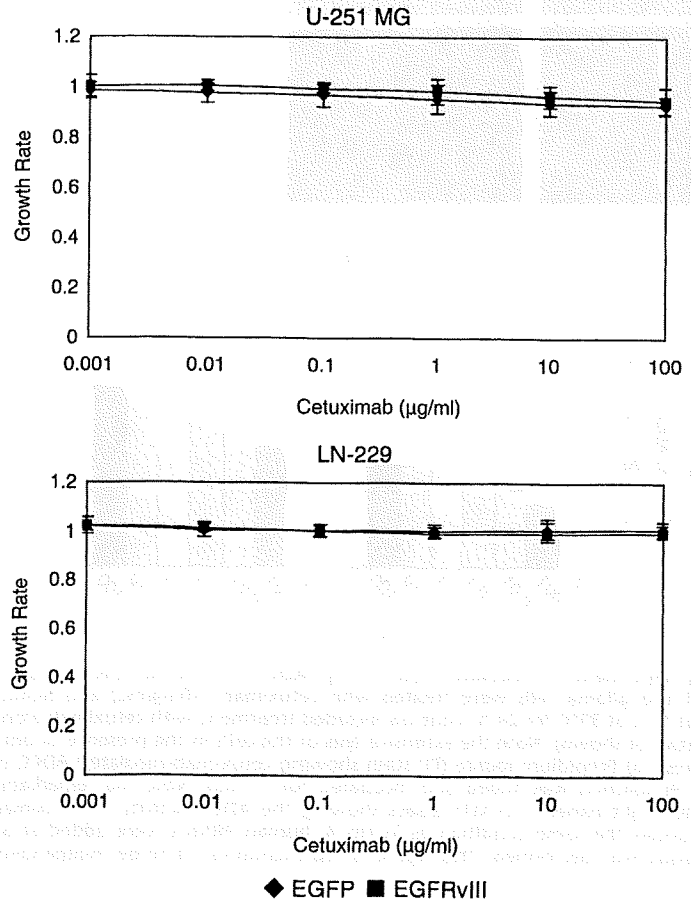

Fig. 4. MTS assays showing the growth-inhibitory effects of cetuximab on malignant glioma cells with and without epidermal growth factor receptor variant III (EGFRvIII) overexpression. 3000 glioma cells per well were placed onto a 96-well tissue culture plate and incubated overnight. Cetuximab was added at concentrations of 0–100 μg/mL and incubated for 48 h before an MTS assay was performed. This figure is representative of three independent experiments. Bars, SD.

Cetuximab induces ADCC in the presence of human PBMCs against malignant glioma cells expressing EGFRvIII. In molecular targeting using mAb, ADCC or CDC activity should be considered as one of the potent antitumor mechanisms.[16] First, we investigated the ADCC activity by morphological observation, PI stain, and an MTS assay. As our results in Fig. 5(a) show, cetuximab in the presence of PBMCs induced extensive lysis of the cells in culture. In contrast, treatment with cetuximab alone, human PBMCs alone, or PBMCs plus human IgG control (data not shown), did not apparently induce lysis of the cells. Correspondingly, PI nucleic acid stain revealed remarkable cell death in the cell population treated with cetuximab and PBMCs (Fig. 5b). To further evaluate cetuximab-induced ADCC against EGFRvIII expressed in the cells, we performed the MTS assay in the presence of human PBMCs at an E/T ratio of 10. In the mock control with low expression levels of wt EGFR, mild ADCC activity was detected (Fig. 5c). On the other hand, cetuximab treatment significantly inhibited the proliferation of the EGFRvIII-overexpressing glioma cells in a dose-dependent manner. There was no significant percentage ADCC at the zero μg/mL of cetuximab in the EGFRvIII-expressing cells as well as in mock controls (EGFP), suggesting that both cells could not be susceptible to PBMCs alone. Next, we examined CDC activity against these cells using the MTS assay in the presence of 25% human serum containing human complement. No CDC-mediated cytolytic effect was observed even at the highest concentration of cetuximab tested (data not shown). These results suggest that this mAb also recognizes the EGFRvIII expressed on the cell surfaces and exerts potent ADCC activity against the glioma cells overexpressing this mutant receptor.

Discussion

Overexpression of EGFR can be a promising characteristic as a molecular target for malignant glioma therapy.[12] Malignant gliomas that are wt EGFR–positive may simultaneously overexpress EGFRvIII, which is reported to be associated with aggressive phenotypes and resistance to chemo- and radiotherapy.[2,10,11] Although anti-EGFR mAb cetuximab may play an important role and be hopefully evaluated in preclinical studies, limited

doi: 10.1111/j.1349-7006.2008.00945.x

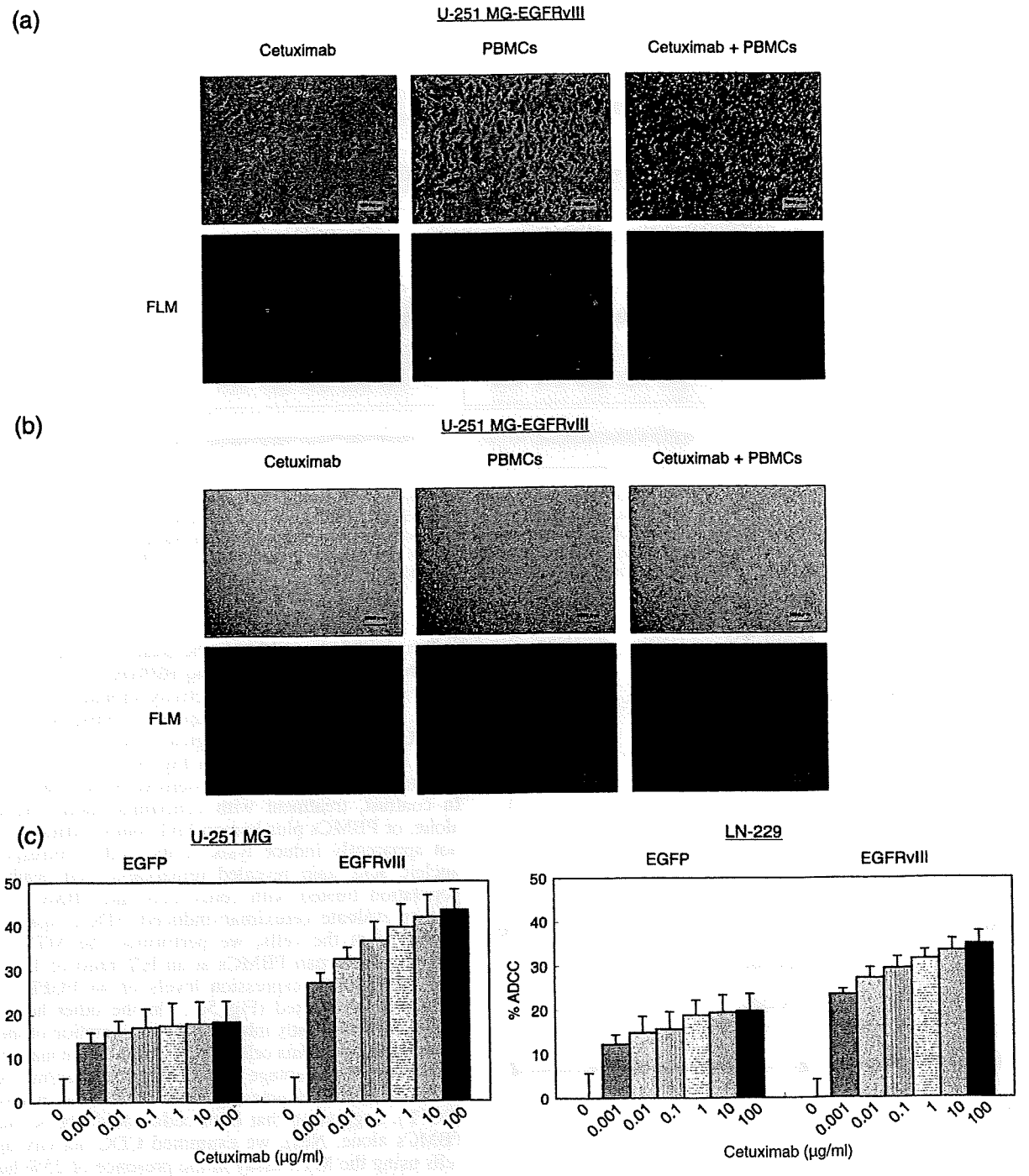

Fig. 5. (a) Microscopic findings showing cetuximab-mediated antibody-dependent cell-mediated cytotoxicity (ADCC) of glioma cells expressing epidermal growth factor receptor variant III (EGFRvIII). Monolayers of the glioma cells were treated with cetuximab (10 μg/mL) and human peripheral blood mononuclear cells (PBMCs) at an effector target ratio of 10:1 at 37°C for 24 h. Controls included treatment with cetuximab alone (left panels), PBMCs alone (middle panels), or PBMCs plus human IgG (data not shown). Note the extensive lysis of the cells in the presence of both cetuximab and PBMC (right panels) but not in any of the control cultures. (b) Propidium iodide (PI) stain showing cetuximab-mediated ADCC of the EGFRvIII-expressing glioma cells. Under the same condition as (a), PI solution was added and incubated for 15 min. Note the remarkable increase of the dead cells in the presence of both cetuximab and PBMC (right panels). (c) MTS assays showing the ADCC activity of cetuximab against malignant glioma cells with and without EGFRvIII expression. Under the same condition as in Fig. 4, human PBMCs were added at an effector target ratio of 10:1 and incubated for 48 h before an MTS assay was performed. This figure is representative of three independent experiments. Bars, SD.

data have been reported regarding the potential of cetuximab to target the EGFRvIII in malignant glioma cells.[3] The present data provide evidence that cetuximab has a capability to recognize EGFRvIII as well as wt EGFR. Although cetuximab produces modest activities to block the EGFRvIII signaling or inhibit the growth of glioma cells with this receptor directly, this mAb has great potential to induce ADCC activity against the EGFRvIII-expressing glioma cells. These results suggest that cetuximab therapy might be effective against malignant gliomas expressing EGFRvIII.

In any anti-EGFR mAb strategy against EGFRvIII, it is of great importance to determine whether or not the mAb can recognize this deletion mutant receptor as the target. EGFR is composed of three major domains: extracellular domains including a ligand-binding site, a hydrophobic transmembrane segment, and a tyrosine-kinase containing cytoplasmic region.[13] EGFRvIII is a mutant form of EGFR encoded by a mutated gene characterized by in-frame deletion of 801 bp coding 6–273 amino acids from the extracellular domain.[11] As the extracellular part is composed of domain I to IV, all of domain I and the amino-terminal 2/3 of domain II are absent in this mutant receptor, while domain III and IV remain intact. Cetuximab has been produced as one of mAbs directed against the extracellular ligand-binding domain of the EGFR, and recent structural studies have demonstrated that the interaction between cetuximab and the EGFR is with domain III of the receptor, not with other domains.[18] Our experiments using immunoprecipitation and immunofluorescence revealed that cetuximab has the ability to bind to EGFRvIII. These findings suggest that EGFRvIII preserves the cetuximab-binding structure regardless of its possible conformational change due to 268 amino acids deletion.[18,23] There have been some recent reports on the possibility of cetuximab for detecting EGFRvIII.[24,25] Aerts *et al.* developed cetuximab-based imaging probe to target EGFR and demonstrated its potential as an imaging agent for not only wild type but also EGFRvIII.[24] Yang's group used cetuximab as a delivery tool of radio-isotope and evaluated boronated mAb for boron neutron capture therapy of a rat glioma expressing either wild-type EGFR or EGFRvIII.[25] This evidence reveals that cetuximab has a potential role in the advancement of anti-EGFR strategy.

Cetuximab competes with ligands for binding to the EGFR.[13] Binding of cetuximab to the EGFR prevents phosphorylation and activation of the receptor tyrosine kinase, resulting in the inhibition of its downstream signal transduction which controls cellular biology.[13,14] This mode of action is considered as the primary mechanism for the antitumor activity of cetuximab. Therefore, EGFRvIII, constitutively activated regardless of ligand-binding, may be insusceptible to such direct inhibition by cetuximab. Indeed, our experiments demonstrated that cetuximab, despite binding to the EGFRvIII, did not have clear inhibitory effects on the phosphorylation of EGFRvIII, Akt, and MAPK.

In mAb therapies, indirect growth-inhibition by activating host immune effector cells is a hopeful mechanism for antitumor activity.[16] Previously, we found that ADCC activity is a major mode of action of anti-HER2/neu mAb trastuzumab for breast cancer cell lines.[20] Therefore, even though cetuximab alone cannot inhibit the growth of the EGFRvIII-expressing cells in culture, it may have cytolitic potential in the treatment of EGFRvIII-expressing tumors *in vivo* by immunological mechanisms such as ADCC or CDC.[26] ADCC has rarely been discussed as one of the antitumor mechanisms of cetuximab. Recently, it has been reported that this mAb causes EGFR-expressing tumor cells to die through this mode of action and elicits effective ADCC activity against lung, head, and neck cancer.[17,27,28] In the literature, the authors describe the potential of cetuximab to exhibit ADCC activity mediated by targeting EGFR expressed in tumor cells, but do not discuss in detail whether cetuximab-mediated ADCC can be evoked against mutant EGFR, especially a deletion mutant form of extracellular domain that is vital for cetuximab binding, which is often discussed in malignant glioma. Our *in vitro* study showed that in the presence of human PBMCs, cetuximab induced strong ADCC, presumably due to additional activation of the immune effector functions by this antibody. A new insight drawn from our study is that even though the target is EGFRvIII, which has a partial deletion of EGF-binding site, once cetuximab binds to the mutant receptor, ADCC could be substantially produced against malignant glioma cells. These findings suggest that *in vivo* treatment of cetuximab could generate antitumor activity through ADCC even against malignant gliomas expressing EGFRvIII, although it should be considered that the growth advantage conferred by EGFRvIII is mostly found *in vivo*, not *in vitro*.

Previous studies have shown that cetuximab binding results in internalization of the antibody-receptor complex, which leads to down-regulation of EGFR expression on the cell surface and the blockading of its downstream signaling.[13] Patel and colleagues examined the ability of cetuximab as an effective drug for EGFRvIII-expressing tumor cells and concluded that down-regulation of EGFRvIII resulted in inhibition of cell proliferation.[29] In our experimental conditions, cetuximab treatment attenuated EGFRvIII expression in a dose-dependent manner. However, despite the decreased levels of this mutant receptor, cetuximab did not apparently inhibit the phosphorylation of Akt and MAPK and the growth of glioma cells with this receptor. Akt functions in one of the major signaling cascades, the phosphatidylinositol-3-kinase-Akt pathway, and controls the balance between glioma cell survival and apoptosis.[13,30,31] p44/42 MAPK functions in another major cascade, the ras–raf–MAPK pathway, which plays a critical role in cell growth and proliferation.[13] There are several possible mechanisms to explain why cetuximab-mediated attenuation of EGFRvIII did not produce antitumor activity in the EGFRvIII-overexpressing glioma cells. The simplest explanation rests in the possibility that, because the EGFRvIII is not completely depleted even at the highest dose of cetuximab tested, EGFRvIII signaling still exists to maintain its downstream activation. Another potentially related explanation is that once constitutive activation of EGFRvIII is established in a cell, it may be difficult to disturb the constant downstream signaling. In any case, we expected cetuximab-induced ADCC against EGFRvIII-expressing cells and clearly demonstrated that cetuximab binding to EGFRvIII could exhibit ADCC activity, inducing glioma cell death. This evidence might hopefully have an impact in anti-EGFR mAb therapy for malignant glioma.

When discussing the clinical relevance of cetuximab therapy against malignant glioma, there are two major points to be elucidated: (i) delivery of cetuximab to the central nervous system; and (ii) recruitment of immune-effector cells into brain tumors. In chemotherapy for brain tumors including malignant glioma, it is necessary to consider whether the drug can effectively reach the tumor through the blood–brain barrier (BBB). Some encouraging findings regarding this problem have been reported. Eller *et al.* demonstrated that intraperitoneal injection of cetuximab significantly increased median survival in nude mice bearing intracranial xenografts of glioblastoma.[3] Arwert and colleagues showed that intravenous injection of cetuximab resulted in a considerable reduction of intracranial glioma burden.[32] This evidence suggests that systemic administration could achieve effective concentration in the brain. On the other hand, there is some information that intact antibodies do not reach significant levels in malignant gliomas after systemic administration. Therefore, in the clinical practice of mAb therapy for brain tumors, several methods to deliver the agent to tumors have been tried out, such as convection-enhanced delivery with stereotactic infusion-catheter placement and osmotic BBB disruption with selective intra-arterial mannitol infusion, producing promising results. Recently, non-invasive localized delivery of mAb to the mouse brain was reported by magnetic resonance imaging–guided focused ultrasound-BBB disruption.[33] These modalities would enable effective delivery of cetuximab to malignant gliomas in the brain. Next, recruitment of immune-effector cells into the brain tumor is also vital for cetuximab to induce ADCC reaction against malignant glioma. In previous literature on mAb treatment for brain tumors, peritumoral infiltrates of macrophages were shown in mice treated with the mAb which was found to induce ADCC *in vitro*, whereas a paucity of T cells and natural killer cells was also described.[34] Although it should be elucidated

doi: 10.1111/j.1349-7006.2008.00945.x

whether macrophages or microglia would be able to mediate the ADCC in the brain, the promising result in the paper suggested that the mAb-mediated ADCC reaction could be evoked in *in vivo* models, which might be encouraging for cetuximab to produce an effective ADCC activity *in vivo*. In conclusion, the above information provides us with some hope that cetuximab may be used to treat patients with malignant glioma. As the next step, further investigation is needed in a clinical setting.

In summary, we have reported that cetuximab can target EGFRvIII and although this mAb appears to be less effective in direct inhibition of EGFRvIII activity, intervention of effector cells such as human PBMCs can produce antitumor efficacy of cetuximab even against EGFRvIII-expressing glioma cells. In view of the concept that cetuximab has been previously shown to develop chemosensitizing and radiosensitizing effects, the use of this mAb may have great therapeutic potential against malignant gliomas.[3,4] Moreover, conjugation of cytotoxic agents such as drugs or radioisotopes might produce enhanced antitumor activity.[12] Thus, we emphasize that targeted therapy using the anti-EGFR mAb cetuximab could play a significant role in the development of multidisciplinary treatment strategies for these tumors.

Acknowledgments

This work was partially supported by funds from the Third Term Comprehensive 10-Year Strategy for Cancer Control (N.K. and K.F.) and Health and Labor Sciences Grants, Research on Advanced Medical Technology, H17-Pharmaco-006 (N.K. and K.F.).

We thank Brystol-Myers Squibb (cetuximab) for providing the anti-EGFR agents for experimental studies.

References

1 von Deimling A, Louis DN, Wiestler OD. Molecular pathways in the formation of gliomas. *Glia* 1995; **15**: 328–38.
2 Frederick L, Wang XY, Eley G, James CD. Diversity and frequency of epidermal growth factor receptor mutations in human glioblastomas. *Cancer Res* 2000; **60**: 1383–7.
3 Eller JL, Longo SL, Kyle MM, Bassano D, Hicklin DJ, Canute GW. Anti-epidermal growth factor receptor monoclonal antibody cetuximab augments radiation effects in glioblastoma multiforme in vitro and in vivo. *Neurosurgery* 2005; **56**: 155–62.
4 Eller JL, Longo SL, Hicklin DJ, Canute GW. Activity of anti-epidermal growth factor receptor monoclonal antibody C225 against glioblastoma multiforme. *Neurosurgery* 2002; **51**: 1005–14.
5 Sugawa N, Ekstrand AJ, James CD, Collins VP. Identical splicing of aberrant epidermal growth factor receptor transcripts from amplified rearranged genes in human glioblastomas. *Proc Natl Acad Sci USA* 1990; **87**: 8602–6.
6 Wong AJ, Ruppert JM, Bigner SH *et al.* Structural alterations of the epidermal growth factor receptor gene in human gliomas. *Proc Natl Acad Sci USA* 1992; **89**: 2965–9.
7 Nishikawa R, Ji XD, Harmon RC *et al.* A mutant epidermal growth factor receptor common in human glioma confers enhanced tumorigenicity. *Proc Natl Acad Sci USA* 1994; **91**: 7727–31.
8 Batra SK, Castelino-Prabhu S, Wikstrand CJ *et al.* Epidermal growth factor ligand-independent, unregulated, cell-transforming potential of a naturally occurring human mutant EGFRvIII gene. *Cell Growth Differ* 1995; **6**: 1251–9.
9 Huang HS, Nagane M, Klingbeil CK *et al.* The enhanced tumorigenic activity of a mutant epidermal growth factor receptor common in human cancers is mediated by threshold levels of constitutive tyrosine phosphorylation and unattenuated signaling. *J Biol Chem* 1997; **272**: 2927–35.
10 Nagane M, Coufal F, Lin H, Bogler O, Cavenee WK, Huang HJ. A common mutant epidermal growth factor receptor confers enhanced tumorigenicity on human glioblastoma cells by increasing proliferation and reducing apoptosis. *Cancer Res* 1996; **56**: 5079–86.
11 Learn CA, Hartzell TL, Wikstrand CJ *et al.* Resistance to tyrosine kinase inhibition by mutant epidermal growth factor receptor variant III contributes to the neoplastic phenotype of glioblastoma multiforme. *Clin Cancer Res* 2004; **10**: 3216–24.
12 Halatsch ME, Schmidt U, Behnke-Mursch J, Unterberg A, Wirtz CR. Epidermal growth factor receptor inhibition for the treatment of glioblastoma multiforme and other malignant brain tumours. *Cancer Treat Rev* 2006; **32**: 74–89.
13 Harding J, Burtness B. Cetuximab. An epidermal growth factor receptor chimeric human-murine monoclonal antibody. *Drugs Today* 2005; **41**: 107–27.
14 Herbst RS, Shin DM. Monoclonal antibodies to a target epidermal growth factor receptor-positive tumors. *Cancer* 2002; **94**: 1593–611.
15 Wakeling AE. Epidermal growth factor receptor tyrosine kinase inhibitors. *Curr Opin Pharmacol* 2002; **2**: 382–7.
16 Harris M. Monoclonal antibodies as therapeutic agents for cancer. *Lancet Oncol* 2004; **5**: 292–302.
17 Kimura H, Sakai K, Arao T, Shimoyama T, Tamura T, Nishio K. Antibody-dependent cellular cytotoxicity of cetuximab against tumor cells with wild-type or mutant epidermal growth factor receptor. *Cancer Sci* 2007; **98**: 1275–80.
18 Li S, Schmitz KR, Jeffrey PD, Wiltzius JJW, Kussie P, Ferguson KM. Structural basis for inhibition of the epidermal growth factor receptor by cetuximab. *Cancer Cell* 2005; **7**: 301–11.
19 Huang S, Armstrong EA, Benavente S, Chinnaiyan P, Harari PM. Dual-agent molecular targeting of the epidermal growth factor receptor (EGFR): combining anti-EGFR antibody with tyrosine kinase inhibitor. *Cancer Res* 2004; **64**: 5355–62.
20 Naruse I, Fukumoto H, Saijo N, Nishio K. Enhanced anti-tumor effect of trastuzumab in combination with cisplatin. *Jpn J Cancer Res* 2002; **93**: 574–81.
21 Perera RM, Narita Y, Furnari FB *et al.* Treatment of human tumor xenografts with monoclonal antibody 806 in combination with a prototypical epidermal growth factor receptor-specific antibody generates enhanced antitumor activity. *Clin Cancer Res* 2005; **11**: 6390–9.
22 Mishima K, Johns TG, Luwor RB *et al.* Growth suppression of intracranial xenografted glioblastomas overexpressing mutant epidermal growth factor receptors by systemic administration of monoclonal antibody (mAb) 806, a novel monoclonal antibody directed to the receptor. *Cancer Res* 2001; **61**: 5349–54.
23 Garrett TP, McKern NM, Lou M *et al.* Crystal structure of a truncated epidermal growth factor receptor extracellular domain bound to transforming growth factor alpha. *Cell* 2002; **110**: 763–73.
24 Aerts HJ, Dubois L, Hackeng TM *et al.* Development and evaluation of a cetuximab-based imaging probe to target EGFR and EGFRvIII. *Radiother Oncol* 2007; **83**: 326–32.
25 Yang W, Wu G, Barth RF *et al.* Molecular targeting and treatment of composite EGFR and EGFRvIII positive gliomas using boronated monoclonal antibodies. *Clin Cancer Res* 2008; **14**: 883–91.
26 Modjtahedi H, Moscatello DK, Box G *et al.* Targeting of cells expressing wild-type EGFR and type-III mutant EGFR (EGFRvIII) by anti-EGFR MAb ICR62: a two-pronged attack for tumour therapy. *Int J Cancer* 2003; **105**: 273–80.
27 Kurai J, Chikumi H, Hashimoto K *et al.* Antibody-dependent cellular cytotoxicity mediated by cetuximab against lung cancer cell lines. *Clin Cancer Res* 2007; **13**: 1552–61.
28 Astsaturov I, Cohen RB, Harari P *et al.* EGFR-targeting monoclonal antibodies in head and neck cancer. *Curr Cancer Drug Targets* 2007; **7**: 650–65.
29 Patel D, Lahiji A, Patel S *et al.* Monoclonal antibody cetuximab binds to and down-regulates constitutively activated epidermal growth factor receptor vIII on the cell surface. *Anticancer Res* 2007; **27**: 3355–66.
30 Matar P, Rojo F, Cassia R *et al.* Combined epidermal growth factor receptor targeting with the tyrosine kinase inhibitor gefitinib (ZD1839) and the monoclonal antibody cetuximab (IMC-C225): superiority over single-agent receptor targeting. *Clin Cancer Res* 2004; **10**: 6487–501.
31 Mellinghoff IK, Wang MY, Vivanco I *et al.* Molecular determinants of the response of glioblastomas to EGFR kinase inhibitors. *N Engl J Med* 2005; **353**: 2012–24.
32 Arwert E, Hingtgen S, Figueiredo J-L *et al.* Visualizing the dynamics of EGFR activity and antiglioma therapies *in vivo*. *Cancer Res* 2007; **67**: 7335–42.
33 Kinoshita M, McDannold N, Jolesz FA, Hynynen K. Noninvasive localized delivery of Herceptin to the mouse brain by MRI-guided focused ultrasound-induced blood–brain barrier disruption. *Proc Nat Acad Sci USA* 2006; **103**: 11 719–23.
34 Sampson JH, Crotty LE, Lee S *et al.* Unarmed, tumor-specific monoclonal antibody effectively treats brain tumors. *Proc Nat Acad Sci USA* 2000; **103**: 11 719–23.

Novel SN-38–Incorporated Polymeric Micelle, NK012, Strongly Suppresses Renal Cancer Progression

Makoto Sumitomo,[1] Fumiaki Koizumi,[2] Takako Asano,[1] Akio Horiguchi,[1] Keiichi Ito,[1] Tomohiko Asano,[1] Tadao Kakizoe,[3] Masamichi Hayakawa,[1] and Yasuhiro Matsumura[4]

[1]Department of Urology, National Defense Medical College, Tokorozawa, Saitama, Japan; [2]Shien-Lab, Medical Oncology, National Cancer Center Hospital; [3]National Cancer Center, Tokyo, Japan; and [4]Investigative Treatment Division, Research Center for Innovative Oncology, National Cancer Center Hospital East, Chiba, Japan

Abstract

It has been recently reported that NK012, a 7-ethyl-10-hydroxy-camptothecin (SN-38)–releasing nanodevice, markedly enhances the antitumor activity of SN-38, especially in hypervascular tumors through the enhanced permeability and retention effect. Renal cell carcinoma (RCC) is a typical hypervascular tumor with an irregular vascular architecture. We therefore investigated the antitumor activity of NK012 in a hypervascular tumor model from RCC. Immunohistochemical examination revealed that Renca tumors contained much more CD34-positive neovessels than SKRC-49 tumors. Compared with CPT-11, NK012 had significant antitumor activity against both bulky Renca and SKRC-49 tumors. Notably, NK012 eradicated rapid-growing Renca tumors in 6 of 10 mice, whereas it failed to eradicate SKRC-49 tumors. In the pulmonary metastasis treatment model, an enhanced and prolonged distribution of free SN-38 was observed in metastatic lung tissues but not in nonmetastatic lung tissues after NK012 administration. NK012 treatment resulted in a significant decrease in metastatic nodule number and was of benefit to survival. Our study shows the outstanding advantage of polymeric micelle-based drug carriers and suggests that NK012 would be effective in treating disseminated RCCs with irregular vascular architectures. [Cancer Res 2008;68(6):1631–5]

Introduction

Passive targeting of the drug delivery system is suited to combating the pathophysiologic characteristics present in many solid tumors: hypervascularity, irregular vascular architecture, potential for secretion of vascular permeability factors, and the absence of effective lymphatic drainage that prevents efficient clearance of macromolecules. These characteristics, unique to solid tumors, are believed to be the basis of the enhanced permeability and retention (EPR) effect (1). Polymeric micelle-based anticancer drugs have recently been developed (2, 3), and some were put under evaluation for clinical trials (4, 5).

7-Ethyl-10-hydroxy-camptothecin (SN-38), a biological active metabolite of irinotecan hydrochloride (CPT-11), has potent antitumor activity, but has not been used clinically because it is a water-insoluble drug. It has been recently shown that novel SN38-incorporated polymeric micelles, NK012, have the potential to allow effective sustained release of SN-38 inside a tumor and possess potent antitumor activities especially in a vascular endothelial growth factor (VEGF)–secreting hypervascular tumor (6), because the supramolecular structures of NK012 which enable SN-38 to accumulate in the target tissue are based on the EPR effect (1).

Renal cell carcinoma (RCC) is a typical hypervascular tumor with an irregular vascular architecture. We therefore conducted an investigation to determine whether NK012 would be effective in treating RCC by using established RCC tumor models with pulmonary metastasis.

Materials and Methods

Drugs and cells. CPT-11 was purchased from Yakult Honsha Co., Ltd. SN-38 and NK012 was prepared and supplied by Nippon Kayaku Co., Ltd. (6). Five human RCC lines (SKRC-49, Caki-1, 769P, 786O, and KU19-20) and murine Renca cells were maintained in DMEM or MEM supplemented with 2 mmol/L glutamine, 1% nonessential amino acids, 100 units/mL streptomycin and penicillin, and 10% FCS.

***In vitro* growth inhibition assay.** The growth inhibitory effects of NK012, SN-38, and CPT-11 were examined with a 3-(4, 5-dimethylthiazol-2-yl)-2, 5-diphenyltetrazolium bromide (MTT) assay, as described previously (6).

***In vivo* growth inhibition assay.** The animal experimental protocols were approved by the Committee for Ethics of Animal Experimentation, and the experiments were conducted in accordance with the Guidelines for Animal Experiments in the National Cancer Center. Athymic nude mice (3–4 wk old) were maintained in a laminar air flow cabinet under aseptic conditions. 10^7 RCC cells were s.c. injected into the backs of the mice. NK012 at doses of 10 mg/kg/d or 20 mg/kg/d and CPT-11 at doses of 15 mg/kg/d or 30 mg/kg/d were given i.v. on days 0 (when tumors were allowed to grow until they became massive in size, around 1.5 cm), 4, and 8. Tumor volume was determined by direct measurement with calipers and calculated as $\pi/6 \times (\text{large diameter}) \times (\text{small diameter})^2$.

Assessment of treatment effects of NK012 on murine pulmonary metastasis model. A total of 1×10^5 Renca cells were inoculated into male BALB/c mice via the tail vein. The mice were randomly divided into three groups of 10. NK012 at dose of 20 mg/kg/d and CPT-11 at dose of 30 mg/kg/d were given i.v. on days 0 (7 d after inoculation), 4, and 8. After that, the mice were sacrificed, their lungs were stained intratracheally with 15% India black ink solution, and the number of metastatic nodules in each mouse was counted. To determine the effect of NK012 on survival, an identical experiment to the one described above was done. After treatment, mice were maintained until each animal showed signs of morbidity (i.e., over 10% weight loss compared with untreated controls), at which point they were sacrificed. Kaplan-Meier analysis was done to determine the effect on time to morbidity, and statistical differences were ranked according to a Mantel-Cox log-rank test using the StatView 5.0 software package.

Histologic and immunohistochemical analysis. Histologic sections were taken from Renca tumor tissues. After extirpation, tissues were fixed with 3.9% formalin in PBS (pH 7.4), and the subsequent preparations and H&E staining were performed by Tokyo Histopathological Laboratory Co.,

Requests for reprints: Yasuhiro Matsumura, Investigative Treatment Division, Research Center for Innovative Oncology, National Cancer Center Hospital East, 6-5-1 Kashiwanoha, Kashiwa City, Chiba 277-8577, Japan. Phone: 81-4-7134-6857; Fax: 81-4-7134-6857; E-mail: yhmatsum@east.ncc.go.jp.

doi:10.1158/0008-5472.CAN-07-6532

Table 1. *In vitro* growth inhibitory activity of SN-38, NK012, and CPT-11 in RCC lines (MTT assay)

Cell line	IC_{50} (μmol/L)		
	SN-38	NK012*	CPT-11
SKRC-49	0.0064 ± 0.005	0.011 ± 0.008	4.14 ± 0.45
Caki-1	0.0062 ± 0.009	0.032 ± 0.006	8.45 ± 0.85
769P	0.015 ± 0.007	0.085 ± 0.014	34.54 ± 3.76
786O	0.031 ± 0.007	0.12 ± 0.012	28.14 ± 1.21
KU19-20	0.10 ± 0.006	0.34 ± 0.014	32.65 ± 1.25
Renca	0045 ± 0.005	0.0096 ± 0.008	2.26 ± 0.05

*The dose of NK012 is expressed as a dose equivalent to SN-38.

Ltd. Monoclonal anti-CD34 antibody (HyCult Biotechnology) was used to detect the tumor blood vessels. CD34-positive neovessels were counted in 10 high-power fields (×400) by two independent investigators who operated in a blinded fashion.

Assay for free (polymer-unbound) SN-38 in lung tissues. The Renca pulmonary metastasis model described above was used for the analysis of the biodistribution of NK012 and CPT-11. Ten days after Renca inoculation, NK012 (20 mg/kg) or CPT-11 (30 mg/kg) was given i.v. to the mice. The mice were sacrificed at 0, 24, 48, and 72 h after administration, and lung samples were taken and stored at −80°C until analysis. We prepared control mice without Renca inoculation as the nonmetastatic model; NK012 was administrated as well, and lung samples were stored. Samples were then homogenized on ice using a Digital homogenizer (Iuchi) and suspended in the mixture of 100 mmol/L glycine-HCl buffer (pH 3)/methanol (1:1, v/v) at a concentration of 5% w/w. Proteins were precipitated with an ice-cold mixture of 1 mmol/L H_3PO_4/MeOH/H_2O (1:1:4, v/v/v) containing camptothecin as an I.S. The sample was vortexed for 10 s and filtered through a MultiScreen Solvinert (Millipore Corporation), and the concentration of free SN-38 in the aliquots of the homogenates (100 μL) was determined using the high-performance liquid chromatography method (6).

Statistical analysis. Data were expressed as mean ± SD. Significance of differences was calculated using the unpaired *t* test with repeated measures of StatView 5.0. $P < 0.05$ was regarded as statistically significant.

Results and Discussion

We first evaluated *in vitro* cellular sensitivity of RCC lines to SN-38, NK012, and CPT-11. The IC_{50} values of each agent for RCC lines are shown in Table 1. NK012 exhibited higher cytotoxic effect against each cell line compared with CPT-11 (96-fold to 406-fold sensitive).

It is essential to elucidate the correlation between the effectiveness of micellar drugs and tumor hypervascularity and hyperpermeability. Gross evaluation of those RCC tumors s.c. injected into the backs of mice revealed that Renca tumors were more reddish and grew faster than SKRC-49 tumors, and immunohistochemical examination showed that Renca tumors contained much more CD34-positive neovessels than SKRC-49 tumors (Fig. 1).

We allowed the tumors to grow until they became massive, around 1.5 cm, and then initiated treatment. A striking decrease in Renca tumor volume was observed on day 15 in mice treated with NK012 at 20 mg/kg/d compared with the untreated control (Fig. 2*A*). Renca bulky masses completely disappeared on day 21 in 6 of 10 mice treated with NK012 at 20 mg/kg/d. On the other hand, Renca tumors in mice treated with CPT-11 at 30 mg/kg/d were not eradicated and rapidly regrew after a partial response at day 15. An approximate 10% body weight loss occurred in mice treated with NK012 20 mg/kg, compared with the untreated controls, but there was no significant difference in comparison with tumor-free mice treated with NK012, suggesting that the decrease in body weight was likely to be due to tumor shrinkage rather than toxic effects. We next compared the antitumor activities of the NK012 and CPT-11 treatment in SKRC-49 and Renca tumors. The SKRC-49 tumor volume in mice treated with NK012 at 20 mg/kg/d on day 21 was over 70% smaller than in the untreated controls on day 21 and ~50% smaller than in mice on day 0 (Fig. 2*B*). However, the SKRC-49 tumors were not eradicated in mice treated with NK012. Considering that equivalent *in vitro* growth inhibitory effects by NK012 were observed for SKRC-49 and Renca cells (Table 1), our results suggest that the antitumor activity of NK012 *in vivo* might be affected by tumor environment factors, such as tumor vascularity.

We next examined the distribution of free SN-38 in the metastatic or nonmetastatic (no inoculation of Renca cells) lung tissues after administration of NK012 or CPT-11. In the case of NK012 administration in mice with lung metastasis, free SN-38 was detectable at the concentration of >100 ng/g in metastatic lung tissues with a typical microvascular architecture (Fig. 3*A*) even at 72 hours after administration, whereas the concentrations of free SN-38 in nonmetastatic lung tissues after NK012 administration were much lower than those in metastatic lung tissues after treatment with NK012 (significant at 24, 48, and 72 hours; $P < 0.05$;

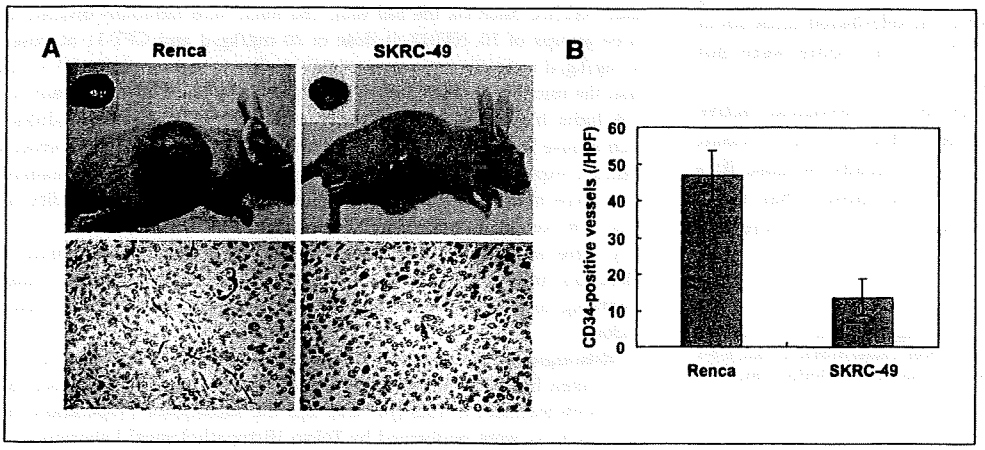

Figure 1. Comparison of tumor angiogeneses of Renca and SKRC-49 in athymic nude mice. *A*, representative photographs of massive tumors developed from Renca and SKRC-49 at 28 d after s.c. injection (inoculation). Immunohistochemical (CD34, ×400) examinations for each tumor are shown. *B*, tumor neovascularization in each tumor was quantified by counting CD34-positive neovessels. *Bars*, SD. Experiments were repeated twice with similar results.

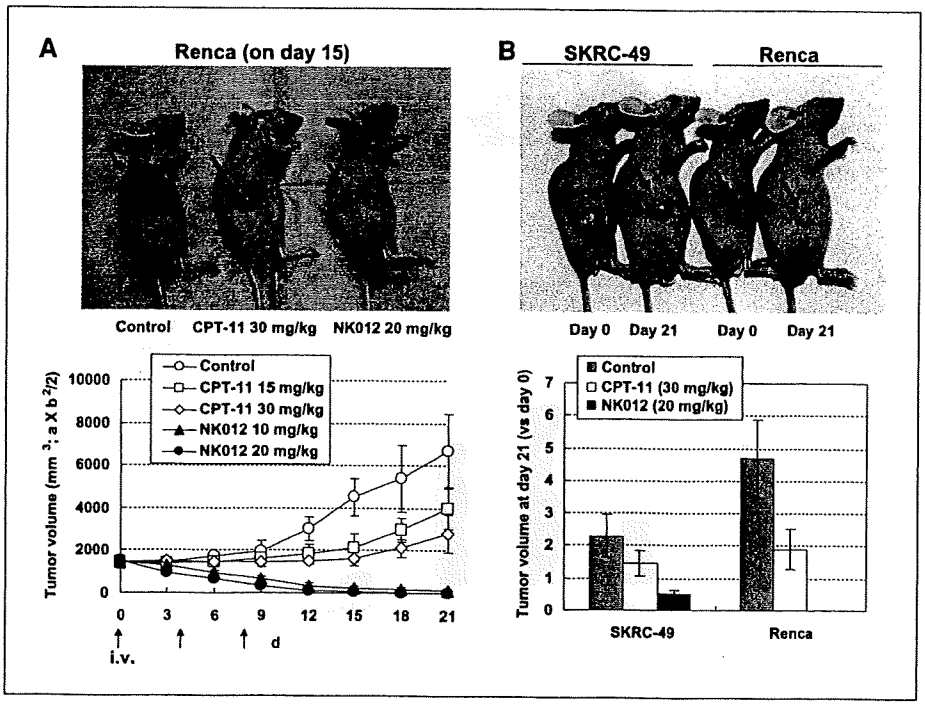

Figure 2. Growth-inhibitory effect of NK012 and CPT-11 on bulky RCC tumors. I.v. administration of NK012 or CPT-11 was started when the mean tumor volumes of groups reached a massive 1,500 mm^3. The mice were divided into test groups as indicated. *A*, representative of each group at day 15 in the Renca allograft model. *Arrows*, Renca allografts (*top*). Time profile of tumor volume in mice treated with NK012 or CPT-11 at indicated doses (*bottom*). Each group consisted of 10 mice. *Bars*, SD. *B*, the comparison of antitumor activities of CPT-11 and NK012 in SKRC-49 xenografts and Renca allografts. Representative of mice treated with NK012 at day 0 and day 21. Experiments were repeated twice with similar results. The mice at day 0 in the photograph belong to the group in the second experiment which started just at day 21 of the first experiment. *Arrows*, tumor grafts. The relative tumor volume values at day 21 to those at day 0 in each group set to 1 (*bottom*). Each group consisted of 10 mice.

Fig. 3*B*). On the other hand, the concentrations of free SN-38 after administration of CPT-11 were almost negligible in metastatic lung tissues at all time points (data not shown). These results strongly suggest that SN-38 could be selectively released from NK012 and maintained in metastatic Renca tumor tissues.

Deviating from the ordinary experimental pulmonary metastasis prevention model, we initiated treatment 7 days after inoculation (day 0) when multiple lung nodules derived from Renca were observed in all mice in our preliminary study (Fig. 4*A*). On day 21, there was no significant difference between the mean number of metastatic nodules in the control group (287 ± 56 nodules, $n = 10$) and in the group receiving CPT-11 treatment (236 ± 59 nodules, $n = 10$). Significant treatment effects were found, however, in the group receiving NK012 treatment (32 ± 18 nodules, $n = 10$) on day 21 compared with the control group on day 21 ($P < 0.0001$). Notably, a dramatic decrease in metastatic nodule number was observed in the NK012 treatment group on day 21 compared with the control group on day 0 (126 ± 23 nodules, $n = 10$, $P < 0.001$; Fig. 4*A*). Kaplan-Meier analysis showed that a significant survival benefit was obtained in the NK012 treatment group compared with

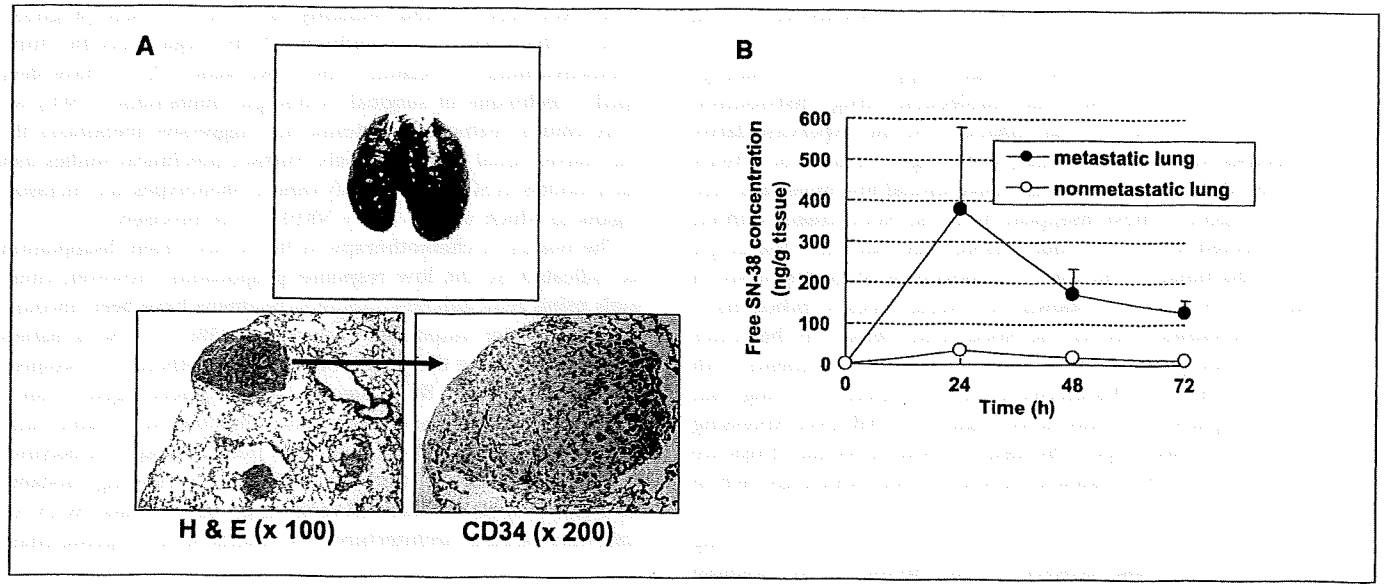

Figure 3. Pulmonary metastasis of Renca cells and lung tissue distribution of free SN-38 after administration of NK012 and CPT-11. *A*, gross appearances of pulmonary metastasis observed 7 d after Renca inoculation (*top*). Multiple metastatic nodules and neovascularization in metastatic lung tumor lesion (*bottom*). *B*, time profile of free SN-38 concentration in metastatic or nonmetastatic lung tissues in mice treated with NK012 (20 mg/kg/d). *Bars*, SD. Experiments were performed in tetraplicate.

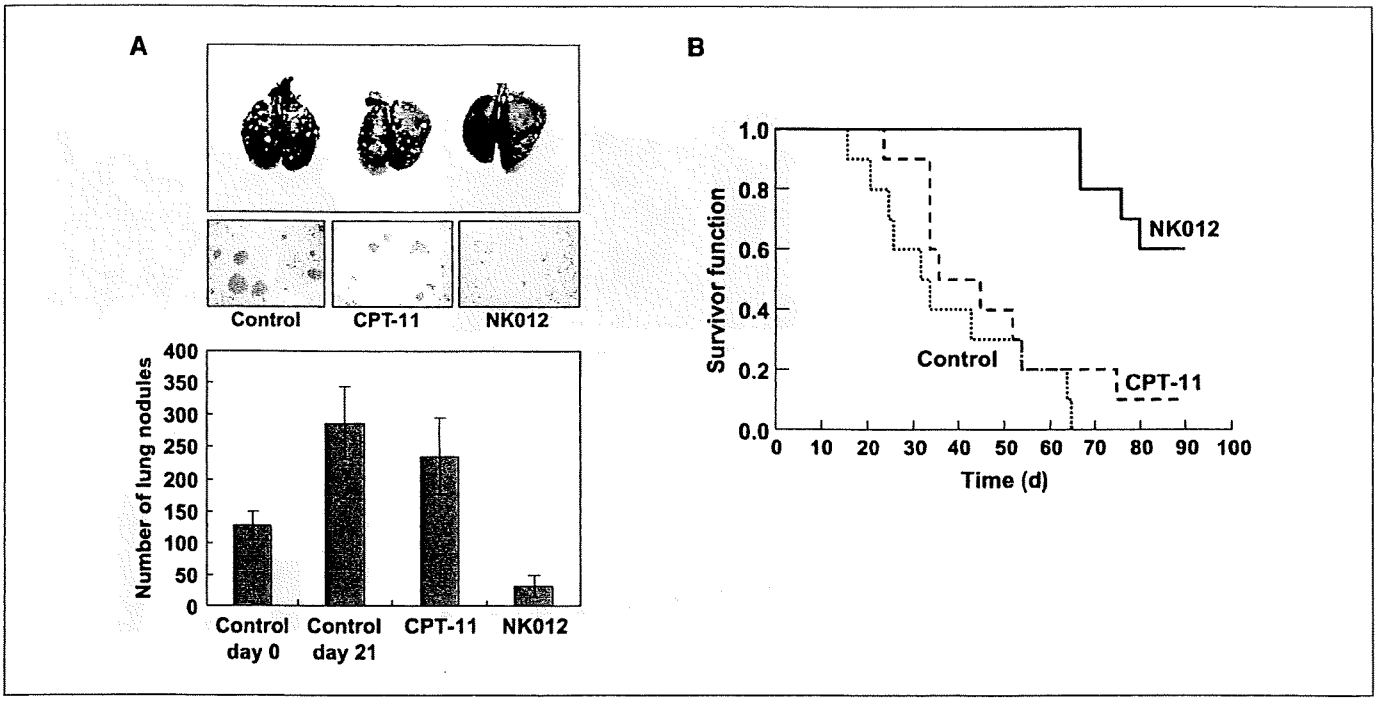

Figure 4. Treatment effect of NK012 on established pulmonary metastasis and survival. NK012 (20 mg/kg/d) and CPT-11 (30 mg/kg/d) were given i.v. to mice with established pulmonary metastasis on days 0 (7 d after Renca inoculation), 4, and 8. *A*, gross and histologic appearances of pulmonary metastases at day 21 (*top*). The metastatic nodules in each mouse were counted. Each group consisted of five mice. *B*, mice were maintained for 90 d after each treatment and survival was assessed by a Kaplan-Meier analysis. Each group consisted of five mice. Experiments were repeated twice with similar results.

the control group ($P < 0.001$), but no significant survival benefit was obtained in CPT-11 treatment group ($P = 0.239$; Fig. 4*B*). Although no severe toxic effects were observed in any mouse treated with NK012, 3 of 10 mice treated with NK012 were sacrificed during the observation period according to the 'Guidelines for Animal Experiments because their body weights had become 10% lower than those of the other mice. However, the sacrificed mice were a little bit smaller than others when they started treatment, and they showed no disseminated lung metastasis (data not shown).

Our results presented here strongly support recent findings reported by us that the macromolecular drug distribution throughout the tumor site was enhanced by the hypervascularity and hyperpermeability, and subsequently higher antitumor activity was achieved (6). We assume that conventional low molecular size anticancer agents almost disappear from the bloodstream without being subjected to the EPR effect before they can reach the target organs (solid tumor). The clinical importance of angiogenesis in human tumors has been shown in several reports indicating a positive relationship between the blood vessel density in the tumor mass and poor prognosis with chemoresistance in patients with various cancers (7–9). Furthermore, recent reports showing that anticancer agents were less active against VEGF-overexpressing tumors (10, 11) may support the idea that low-molecular drugs are not so effective in the treatment of solid tumors which are rich in blood vessels.

Our study thus far has several limitations about clarifying whether extensive angiogenesis in the tumor is an essential determinant for the susceptibility to NK012. In our ongoing study, we found that NK012 also has a striking antitumor activity against some hypovascular tumor models of human pancreatic cancer xenografts.[5] It also remains unclear whether NK012 possesses strong antitumor activity in other metastatic sites besides the lung. It is known that the EPR effect is affected by various permeability factors, such as bradykinin (12), nitric oxide (13). and various cytokines independent of VEGF and hypervascularity (14). Among solid tumors with rapid progression potential, irregularity occurs not only in blood flow and vascular density, but also in the vascular network and anatomic architecture (15, 16), suggesting that EPR effect may be predominantly promoted in rapid-progressive tumor phenotypes and influenced by organ-specific tumor microenvironment. Hoffman and coworkers (17, 18) have developed a technique of surgical orthotopic implantation (SOI) with more clinical features of systemic and aggressive metastases than our conventional animal models. Further preclinical studies using such models as SOI might clarify cancer phenotypes and metastatic organs to which we can apply NK012 more precisely.

The results of chemotherapy in RCCs have been disappointing, as indicated by the low response proportions. However, clinical trials using gemcitabine-containing regimens have been encouraging, with major responses occurring in 5% to 17% of patients (19, 20), suggesting the possibility that chemotherapy is promising as a modality for RCC therapy if anticancer agents can be selectively delivered, released, and maintained around tumor tissues. Our current report highlights the advantages of polymeric micelle-based drug carriers like NK012 as promising modalities for treatment, rather than prevention, of disseminated RCCs with abnormal vascular architecture. The results of our ongoing phase-I

[5] Y. Saito, M. Yasumaga, J. Kuroda, Y. Koga, and Y. Matsumura. Unpublished data.

clinical trial and future phase-II trials of NK012 in patients with advanced solid tumors including RCC might meet or even exceed our expectations.

Acknowledgments

Received 12/10/2007; revised 1/25/2008; accepted 1/31/2008.

Grant support: Grant-in-aid from 3rd Term Comprehensive Control Research for Cancer, Ministry of Health, Labor and Welfare (Y. Matsumura) and Scientific Research on Priority Areas from the Ministry of Education, Culture, Sports, Science and Technology (Y. Matsumura).

The costs of publication of this article were defrayed in part by the payment of page charges. This article must therefore be hereby marked *advertisement* in accordance with 18 U.S.C. Section 1734 solely to indicate this fact.

We thank H. Miyatake and N. Mie for their technical assistance and K. Shiina for her secretarial assistance.

References

1. Matsumura Y, Maeda H. A new concept for macromolecular therapeutics in cancer chemotherapy: mechanism of tumoritropic accumulation of proteins and the antitumor agent smancs. Cancer Res 1986;46:6387–92.
2. Yokoyama M, Miyauchi M, Yamada N, et al. Characterization and anticancer activity of the micelle-forming polymeric anticancer drug adriamycin-conjugated poly(ethylene glycol)-poly(aspartic acid) block copolymer. Cancer Res 1990;50:1693–700.
3. Kataoka K, Harada A, Nagasaki Y. Block copolymer micelles for drug delivery: design, characterization and biological significance. Adv Drug Deliv Rev 2001;47:113–31.
4. Matsumura Y, Hamaguchi T, Ura T, et al. Phase I clinical trial and pharmacokinetic evaluation of NK911, a micelle-encapsulated doxorubicin. Br J Cancer 2004;91:1775–81.
5. Hamaguchi T, Kato K, Yasui H, et al. A phase I and pharmacokinetic study of NK105, a paclitaxel-incorporating micellar nanoparticle formulation. Br J Cancer 2007;97:170–6.
6. Koizumi F, Kitagawa M, Negishi T, et al. Novel SN-38-incorporating polymeric micelles, NK012, eradicate vascular endothelial growth factor-secreting bulky tumors. Cancer Res 2006;66:10048–56.
7. Gasparini G, Harris AL. Clinical importance of the determination of tumor angiogenesis in breast carcinoma: much more than a new prognostic tool. J Clin Oncol 1995;13:765–82.
8. Takahashi Y, Kitadai Y, Bucana CD, Cleary KR, Ellis LM. Expression of vascular endothelial growth factor and its receptor, KDR, correlates with vascularity, metastasis, and proliferation of human colon cancer. Cancer Res 1995;55:3964–8.
9. Williams JK, Carlson GW, Cohen C, Derose PB, Hunter S, Jurkiewicz MJ. Tumor angiogenesis as a prognostic factor in oral cavity tumors. Am J Surg 1994;168:373–80.
10. Natsume T, Watanabe J, Koh Y, et al. Antitumor activity of TZT-1027 (Soblidotin) against vascular endothelial growth factor-secreting human lung cancer *in vivo*. Cancer Sci 2003;94:826–33.
11. Zhang L, Hannay JA, Liu J, et al. Vascular endothelial growth factor overexpression by soft tissue sarcoma cells: implications for tumor growth, metastasis, and chemoresistance. Cancer Res 2006;66:8770–8.
12. Matsumura Y, Maruo K, Kimura M, Yamamoto T, Konno T, Maeda H. Kinin-generating cascade in advanced cancer patients and *in vitro* study. Jpn J Cancer Res 1991;82:732–41.
13. Wu J, Akaike T, Hayashida K, et al. Identification of bradykinin receptors in clinical cancer specimens and murine tumor tissues. Int J Cancer 2002;98:29–35.
14. Maeda H, Fang J, Inutsuka T, Kitamoto Y. Vascular permeability enhancement in solid tumor: various factors, mechanisms involved and its implications. Int Immunopharmacol 2003;3:319–28.
15. Suzuki M, Takahashi T, Sato T. Medial regression and its functional significance in tumor-supplying host arteries. A morphometric study of hepatic arteries in human livers with hepatocellular carcinoma. Cancer 1987;59:444–50.
16. Skinner SA, Tutton PJ, O'Brien PE. Microvascular architecture of experimental colon tumors in the rat. Cancer Res 1990;50:2411–7.
17. An Z, Jiang P, Wang X, Moossa AR, Hoffman RM. Development of a high metastatic orthotopic model of human renal cell carcinoma in nude mice: benefits of fragment implantation compared to cell-suspension injection. Clin Exp Metastasis 1999;17:265–70.
18. Hoffman RM. Orthotopic metastatic mouse models for anticancer drug discovery and evaluation: a bridge to the clinic. Invest New Drugs 1999;17:343–59.
19. Rini BI, Vogelzang NJ, Dumas MC, Wade JL III, Taber DA, Stadler WM. Phase II trial of weekly intravenous gemcitabine with continuous infusion fluorouracil in patients with metastatic renal cell cancer. J Clin Oncol 2000;18:2419–26.
20. Nanus DM, Garino A, Milowsky MI, Larkin M, Dutcher JP. Active chemotherapy for sarcomatoid and rapidly progressing renal cell carcinoma. Cancer 2004;101:1545–51.

Int. J. Cancer: **122,** 2148–2153 (2008)

Synergistic antitumor activity of the novel SN-38-incorporating polymeric micelles, NK012, combined with 5-fluorouracil in a mouse model of colorectal cancer, as compared with that of irinotecan plus 5-fluorouracil

Takako Eguchi Nakajima[1,2], Masahiro Yasunaga[2], Yasuhiko Kano[3], Fumiaki Koizumi[4], Ken Kato[1], Tetsuya Hamaguchi[1], Yasuhide Yamada[1], Kuniaki Shirao[1], Yasuhiro Shimada[1] and Yasuhiro Matsumura[2]*

[1]*Gastrointestinal Oncology Division, National Cancer Center Hospital, Tokyo, Japan*
[2]*Investigative Treatment Division, Research Center for Innovative Oncology, National Cancer Center Hospital East, Kashiwa, Chiba, Japan*
[3]*Hematology Oncology, Tochigi Cancer Center, Tochigi, Japan*
[4]*Shien Lab Medical Oncology Division, National Cancer Center Hospital, Tokyo, Japan*

The authors reported in a previous study that NK012, a 7-ethyl-10-hydroxy-camptothecin (SN-38)-releasing nano-system, exhibited high antitumor activity against human colorectal cancer xenografts. This study was conducted to investigate the advantages of NK012 over irinotecan hydrochloride (CPT-11) administered in combination with 5-fluorouracil (5FU). The cytotoxic effects of NK012 or SN-38 (an active metabolite of CPT-11) administered in combination with 5FU was evaluated *in vitro* in the human colorectal cancer cell line HT-29 by the combination index method. The effects of the same drug combinations was also evaluated *in vivo* using mice bearing HT-29 and HCT-116 cells. All the drugs were administered i.v. 3 times a week; NK012 (10 mg/kg) or CPT11 (50 mg/kg) was given 24 hr before 5FU (50 mg/kg). Cell cycle analysis in the HT-29 tumors administered NK012 or CPT-11 *in vivo* was performed by flow cytometry. NK012 exerted more synergistic activity with 5FU compared to SN-38. The therapeutic effect of NK012/5FU was significantly superior to that of CPT-11/5FU against HT-29 tumors ($p = 0.0004$), whereas no significant difference in the antitumor effect against HCT-116 tumors was observed between the 2-drug combinations ($p = 0.2230$). Cell-cycle analysis showed that both NK012 and CPT-11 tend to cause accumulation of cells in the S phase, although this effect was more pronounced and maintained for a more prolonged period with NK012 than with CPT-11. Optimal therapeutic synergy was observed between NK012 and 5FU, therefore, this regimen is considered to hold promise of clinical benefit, especially for patients with colorectal cancer.

Key words: NK012; SN-38; 5-fluorouracil; drug delivery system; colorectal cancer

The 5-year survival rates of colorectal cancer (CRC) have improved remarkably over the last 10 years, accounted for in large part by the extensively investigated agents after 5-fluorouracil (5FU). Irinoetcan hydrochloride (CPT-11), a water-soluble, semi-synthetic derivative of camptothecin, is one such agent that has been shown to be highly effective, and currently represents a key-drug in first- and second-line treatment regimens for CRC. CPT-11 monotherapy, however, has not been shown to yield superior efficacy, including in terms of the median survival time, to bolus 5FU/leucovorin (LV) alone.[1] In 2 Phase III trials, the addition of CPT-11 to bolus or infusional 5FU/LV regimens clearly yielded greater efficacy than administration of 5FU/LV alone, with a doubling of the tumor response rate and prolongation of the median survival time by 2–3 months.[1,2]

CPT-11 is converted to 7-ethyl-10-hydroxy-camptothecin (SN-38), a biologically active and water-insoluble metabolite of CPT-11, by carboxylesterases in the liver and the tumor. SN-38 has been demonstrated to exhibit up to a 1,000-fold more potent cytotoxic activity than CPT-11 against various cancer cells *in vitro*.[3] The metabolic conversion rate is, however, very low, with only <10% of the original volume of CPT-11 being metabolized to SN-38[4,5]; conversion of CPT-11 to SN-38 also depends on genetic interindividual variability of the activity of carboxylesterases.[6] Direct use of SN-38 itself for clinical cancer treatment must be shown to be identical in terms of both efficacy and toxicity.

Some drugs incorporated in drug delivery systems (DDS), such as Abraxane and Doxil, are already in clinical use.[7,8] The clinical benefits of DDS are based on their EPR effect.[9] The EPR effect is based on the pathophysiological characteristics of solid tumor tissues: hypervascularity, incomplete vascular architecture, secretion of vascular permeability factors stimulating extravasation within cancer tissue, and absence of effective lymphatic drainage from the tumors that impedes the efficient clearance of macromolecules accumulated in solid tumor tissues. Several types of DDS can be used for incorporation of a drug. A liposome-based formulation of SN-38 (LE-SN38) has been developed, and a clinical trial to assess its efficacy is now under way.[10,11]

Recently, we demonstrated that NK012, novel SN-38-incorporating polymeric micelles, exerted superior antitumor activity and less toxicity than CPT-11.[12] NK012 is characterized by a smaller size of the particles than LE-SN38; the mean particle diameter of NK012 is 20 nm. NK012 can release SN-38 under neutral conditions even in the absence of a hydrolytic enzyme, because the bond between SN-38 and the block copolymer is a phenol ester bond, which is stable under acidic conditions and labile under mild alkaline conditions. The release rate of SN-38 from NK012 under physiological conditions is quite high; more than 70% of SN-38 is released within 48 hr. We speculated that the use of NK012, in place of CPT-11, in combination with 5FU may yield superior results in the treatment of CRC. In the present study, we evaluated the antitumor activity of NK012 administered in combination with 5FU as compared to that of CPT-11 administered in combination with 5FU against CRC in an experimental model.

Material and methods

Cells and animals

The human colorectal cancer cell lines used, namely, HT-29 and HCT-116, were purchased from the American Type Culture Collection (Rockville, MD). The HT-29 cells and HCT-116 cells were maintained in RPMI 1640 supplemented with 10% fetal bovine serum (Cell Culture Technologies, Gaggenau-Hoerden, Germany), penicillin, streptomycin, and amphotericin B (100 units/mL, 100 μg/mL, and 25 μg/mL, respectively; Sigma, St. Louis, MO) in a humidified atmosphere containing 5% CO_2 at 37°C.

BALB/c *nu/nu* mice were purchased from SLC Japan (Shizuoka, Japan). Six-week-old mice were subcutaneously (s.c.)

***Correspondence to:** Investigative Treatment Division, Research Center for Innovative Oncology, National Cancer Center Hospital East, 6-5-1 Kashiwanoha, Kashiwa, Chiba 277-8577, Japan. Fax: +81-4-7134-6866. E-mail: yhmatsum@east.ncc.go.jp
Received 2 September 2007; Accepted after revision 20 November 2007
DOI 10.1002/ijc.23381
Published online 14 January 2008 in Wiley InterScience (www.interscience.wiley.com).

inoculated with 1×10^6 cells of HT-29 or HCT-116 cell line in the flank region. The length (a) and width (b) of the tumor masses were measured twice a week, and the tumor volume (TV) was calculated as follows: $TV = (a \times b^2)/2$. All animal procedures were performed in compliance with the Guidelines for the Care and Use of Experimental Animals established by the Committee for Animal Experimentation of the National Cancer Center; these guidelines meet the ethical standards required by law and also comply with the guidelines for the use of experimental animals in Japan.

Drugs

The SN-38-incorporating polymeric micelles, NK012, and SN-38 were prepared by Nippon Kayaku (Tokyo, Japan).[12] CPT-11 was purchased from Yakult Honsha (Tokyo, Japan). 5FU was purchased from Kyowa Hakko (Tokyo, Japan).

Cell growth inhibition assay

HT-29 cells were seeded in 96-well plates at a density of 2,000 cells/well in a final volume of 90 μL. Twenty-four hours after seeding, a graded concentration of NK012 or SN-38 was added concurrently with 5FU to the culture medium of the HT-29 cells in a final volume of 100 μL for drug interaction studies. The culture was maintained in the CO_2 incubator for an additional 72 hr. Then, cell growth inhibition was measured by the tetrazolium salt-based proliferation assay (WST assay; Wako Chemicals, Osaka, Japan). WST-1 labeling solution (10 μL) was added to each well and the plates were incubated at 37°C for 3 hr. The absorbance of the formazan product formed was detected at 450 nm in a 96-well spectrophotometric plate reader. Cell viability was measured and compared to that of the control cells. Each experiment was carried out in triplicate and was repeated at least 3 times. Data were averaged and normalized against the nontreated controls to generate dose-response curves.

Drug interaction analysis

The nature of interaction between NK012 or SN-38 and 5FU against HT-29 cells was evaluated by median-effect plot analyses and the combination index (CI) method of Chou and Talalay.[13] Data analysis was performed using the Calcusyn software (Biosoft, NY, USA). NK012 or SN-38 was combined with 5FU at a fixed ratio that spanned the individual IC_{50} values of each drug. The IC_{50} values were determined on the basis of the dose-response curves using the WST assay. For any given drug combination, the CI is known to represent the degree of synergy, additivity or antagonism. It is expressed in terms of fraction-affected (Fa) values, which represents the percentage of cells killed or inhibited by the drug. Isobologram equations and Fa/CI plots were constructed by computer analysis of the data generated from the median effect analysis. Each experiment was performed in triplicate with 6 gradations and was repeated at least 3 times. The resultant dose-response curves were averaged, to create a single composite dose-response curve for each combination.

In vivo analysis of the effects of NK012 combined with 5FU as compared to those of CPT-11 combined with 5FU

When the mean tumor volumes reached ~93 mm^3, the mice were randomly divided into test groups consisting of 5 mice per group (Day 0). The drugs were administered i.v. *via* the tail vein of the mice. In the groups administered NK012 or 5FU as single agents, the drug was administered on Days 0, 7 and 14. In the combined treatment groups, NK012 or CPT-11 was administered 24 hr before 5FU on Days 0, 7 and 14, according to the previously reported combination schedule for CPT-11 and 5FU.[14] Complete response (CR) was defined as tumor not detectable by palpation at 90 days after the start of treatment, at which time-point the mice were sacrificed. Tumor volume and body weight were measured twice a week. As a general rule, animals in which the tumor volume exceeded 2,000 mm^3 were also sacrificed.

Experiment 1. Evaluation of the effects of NK012 combined with 5FU and determination of the maximum tolerated dose (MTD) of NK012/5FU. By comparing the data between NK012 administered as a single agent and NK012/5FU, we evaluated the effects of the combined regimen against the s.c HT-29 tumors. A preliminary experiment showed that combined administration of NK012 15 mg/kg + 5FU 50 mg/kg every 6 days caused drug-related lethality (data not shown). To determine the MTD, therefore, we set the dosing schedule of the combined regimen at 5 or 10 mg/kg of NK012 + 50 mg/kg of 5FU three times a week.

Experiment 2. Comparison of the antitumor effect of NK012/5FU and CPT-11/5FU. Based on a comparison of the data between NK012/5FU and CPT-11/5FU against the s.c. HT-29 and HCT-116 tumors, we investigated the feasibility of the clinical application of NK012/5FU for the treatment of CRC. CPT-11/5FU was administered three times a week at the respective MTDs of the 2 drugs as previously reported, that is, CPT11 at 50 mg/kg and 5FU at 50 mg/kg, respectively.[14] NK012/5FU was administered once three times a week at the respective MTDs of the 2 drugs determined from Experiment 1.

Cell cycle analysis

Samples from the HT-29 tumors that had grown to 80–100 mm^3 were removed from the mice at 6, 24, 48, 72 and 96 hr after the administration of NK012 alone at 10 mg/kg or CPT-11 alone at 50 mg/kg. The samples were excised, minced in PBS and fixed in 70% ethanol at −20°C for 48 hr. They were then digested with 0.04% pepsin (Sigma chemical Co., St Lous, MO) in 0.1 N HCL for 60 min at 37°C in a shaking bath to prepare single-nuclei suspensions. The nuclei were then centrifuged, washed twice with PBS and stained with 40 μg/mL of propidium iodide (Molecular Probes, OR) in the presence of 100 μg/mL RNase in 1 mL PBS for 30 min at 37°C. The stained nuclei were analyzed with B-D FACSCalibur (BD Biosciences, San Jose, CA), and the cell cycle distribution was analyzed using the Modfit program (Verity Software House Topsham, ME).

Statistical analyses

Data were expressed as mean ± SD. Data were analysed with Student's t test when the groups showed equal variances (F test), or Welch's test when they showed unequal variances (F test). $p < 0.05$ was regarded as statistically significant. All statistical tests were 2-sided.

Results

Antiproliferative effects of NK012 or SN-38 administered in combination with 5FU

Figure 1*a* shows the dose-response curves for NK012 alone, 5FU alone and a combination of the two. The IC_{50} levels of NK012 and 5FU against the HT-29 cells were 39 nM and 1 μM, respectively, and the IC_{50} level of SN-38 was 14 nM (data not shown). Based on these data, the molar ratio of NK012 or SN-38:5FU of 1:1,000 was used for the drug combination studies.

Figures 1*b* and 1*c* show the median-effect and the combination index plots. Combination indices (CIs) of <1.0 are indicative of synergistic interactions between 2 agents; additive interactions are indicated by CIs of 1.0, and antagonism by CIs of >1.0. Figure 1*c* shows the combination index for NK012 and 5FU, when 2 drugs are supposed to be mutually exclusive. Marked synergism was observed between Fa 0.2 and 0.6. Theoretically, the CI method is the most reliable around an Fa of 0.5, suggesting synergistic effects of the combination of NK012 and 5FU. This synergistic effect was more evident than that of SN-38/5FU (Fig. 1*d*).

In vivo *effect of combined NK012 and 5FU*

Experiment 1. Dose optimization and effect of combined NK012 and 5FU against HT-29 tumors. Comparison of the relative tumor volumes on Day 40 revealed significant differences between

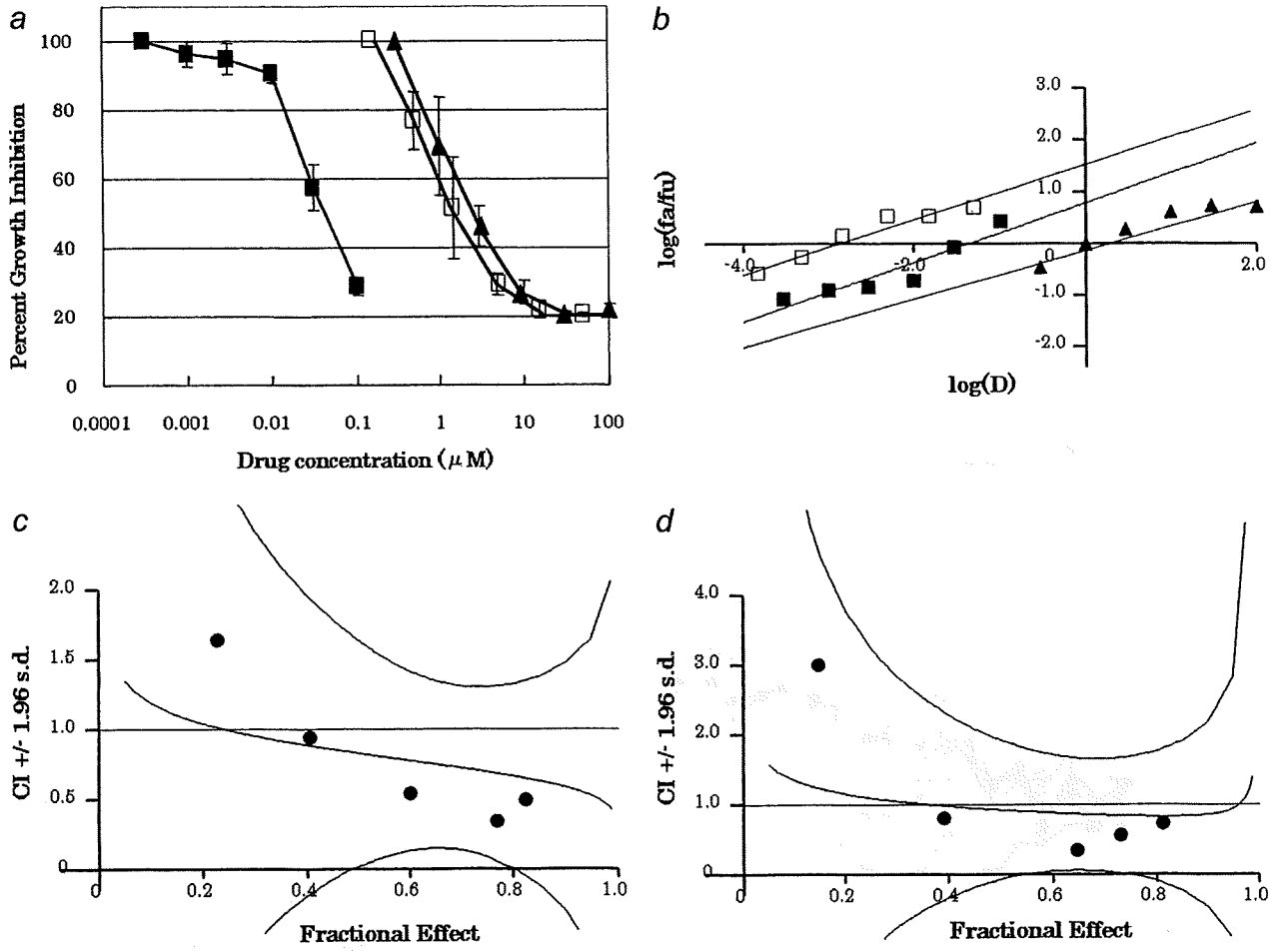

FIGURE 1 – Interaction of NK012 and 5FU *in vitro*. (*a*) Dose-response curves for NK012 alone (■), 5FU alone (▲) and their combination (□) against HT-29 cells. HT-29 cells were seeded at 2,000 cells/well. Twenty-four hours after seeding, a graded concentration of NK012 or 5FU was added to the culture medium of the HT-29 cells. Cell growth inhibition was measured by WST assay after 72 hr of treatment. Cell viability was measured and compared with that of the control cells. Each experiment was carried out independently and repeated at least 3 times. Points, mean of tripricates; bars, SD. (*b*) Median effect plot for the interaction of NK012 and 5FU. (*c*, *d*) Combination index for the interaction as a function of the level of effect (fraction effect = 0.5 is the IC_{50}). The straight line across the CI value of 1.0 indicates additive effect and CIs above and below indicate antagonism and synergism, respectively. The molar ratio of NK012/5FU (*c*) or SN-38/5FU (*d*) at 1:1,000 was tested by CI analysis. Black circles represent the CIs of the actual data points, solid lines represent the computer-derived CIs at effect levels ranging from 10 to 100% inhibition of cell growth, and the dotted lines represent the 95% confidence intervals.

those in the mice administered NK012 alone and those administered NK012/5FU at 5 mg/kg of NK012 ($p = 0.018$) (Fig. 2*a*). Although there was no statistically significant difference in the relative tumor volume measured on Day 54 between the mice administered NK012 alone and NK012/5FU at 10 mg/kg of NK012 ($p = 0.3050$), a trend of superior antitumor effect was demonstrated in the group treated with NK012/5FU at 10 mg/kg of NK012 (Fig. 2*a*). The CR rates were 20, 40 and 60% for 5 mg/kg NK012 + 50 mg/kg 5FU, 10 mg/kg NK012 alone and 10 mg/kg NK012 + 50 mg/kg 5FU, respectively. The schedule of 10 mg/kg NK012 + 50 mg/kg 5FU resulted in no remarkable toxicity in terms of body weight changes, and these doses were determined as representing the MTDs (Fig. 2*b*).

Experiment 2. Comparison of the antitumor effect of combined NK012/5FU and CPT-11/5FU against HT-29 and HCT-116 tumors. The therapeutic effect of NK012/5FU on Day 60 was significantly superior to that of CPT-11/5FU against the HT-29 tumors ($p = 0.0004$) (Fig. 3*a*). A more potent antitumor effect, namely, a 100% CR rate, was obtained in the NK012/5FU group as compared to the 0% CR rate in the CPT-11/5FU group. Although no statistically significant difference in the relative tumor volume on Day 61 was demonstrated between the NK012/5FU and CPT-11/5FU in the case of the HCT-116 tumors ($p = 0.2230$), a trend of superior antitumor effect against these tumors was observed in the NK012/5FU treatment group (Fig. 3*b*). The CR rates for the case of the HCT-116 tumors were 0% in both NK012/5FU and CPT-11/5FU groups.

Specificity of cell cycle perturbation

We studied the differences in the effects between NK012 10 mg/kg and CPT-11 50 mg/kg on the cell cycle (Fig. 4*a*). The data indicated that both NK012 and CPT-11 tended to cause accumulation of cells in the S phase, although the effect of NK012 was stronger and maintained for a more prolonged period than that of CPT-11; the maximal percentage of S-phase cells in the total cell population in the tumors was 34% at 24 hr after the administration of CPT-11, whereas it was 39% at 48 hr after the administration of NK012 (Figs. 4*b*, and 4*c*).

Discussion

Our primary endpoint was to clarify the advantages of NK012 over CPT-11 administered in combination with 5FU. We demonstrated that combined NK012 and 5FU chemotherapy exerts more

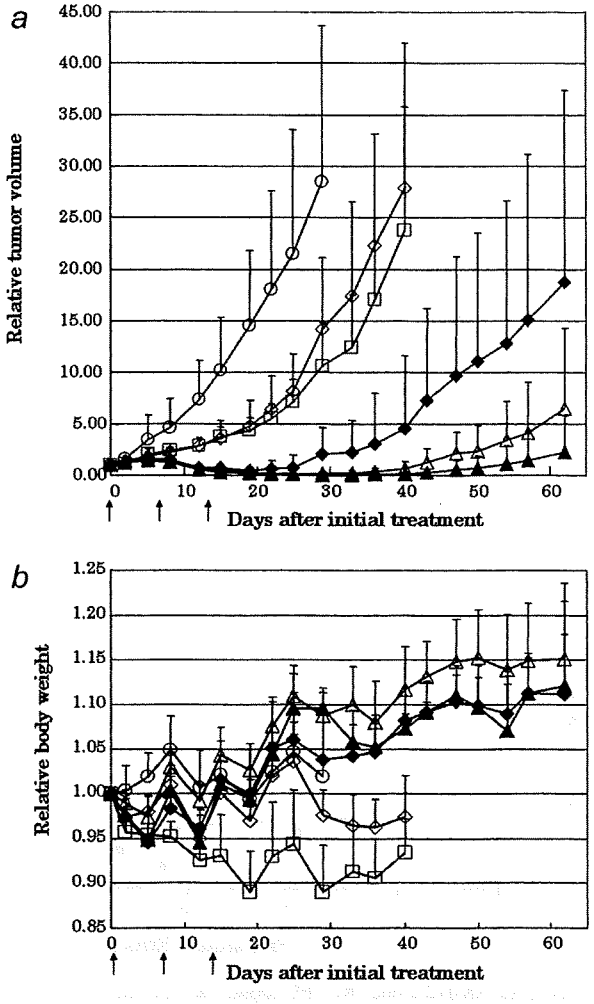

FIGURE 2 – Effect of NK012 alone or NK012 in combination with 5FU against HT-29 tumor-bearing mice. Points, mean; bars, SD. (*a*) Antitumor effect of each regimen on Days 0, 7 and 14. (○) control, (□) 5FU 50 mg/kg alone, (◇) NK012 5 mg/kg alone, (◆) NK012 5 mg/kg 24 hr before 5FU 50 mg/kg, (△) NK012 10 mg/kg alone, (▲) NK012 10 mg/kg 24 hr before 5FU 50 mg/kg. (*b*) Changes in the relative body weight. Data were derived from the same mice as those used in the present study.

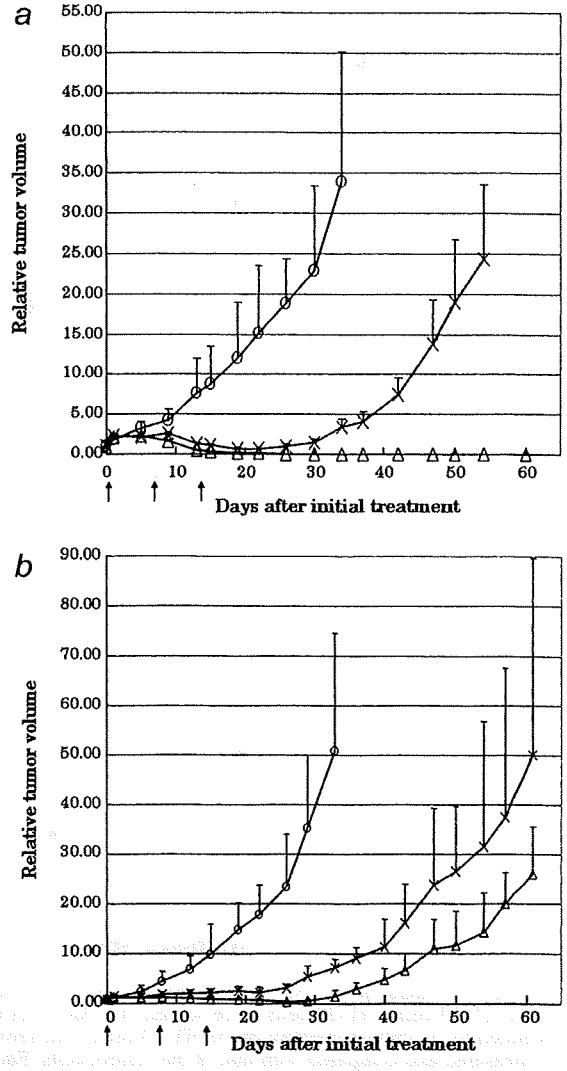

FIGURE 3 – Effect of NK012/5FU as compared with that of CPT11/5FU against HT-29 (*a*) or HCT-116 (*b*) tumor-bearing mice. Antitumor effect of each schedule on Days 0, 7 and 14. (○) control, (×) CPT-11 50 mg/kg 24 hr before 5FU 50 mg/kg, (△) NK012 10 mg/kg 24 hr before 5FU 50 mg/kg. Points, mean; bars, SD.

synergistic activity *in vitro* and significantly greater antitumor activity against human CRC xenografts as compared to CPT-11/5FU. The combination of NK012 and 5FU is considered to hold promise of clinical benefit for patients with CRC.

CPT-11, a topoisomerase-I inhibitor, and 5FU, a thymidilate synthase inhibitor, have been demonstrated to be effective agents for the treatment of CRC. A combination of these 2 drugs has also been demonstrated to be clearly more effective than either CPT-11 or 5FU/LV administered alone *in vivo* and in clinical settings.[1,2,14] Administration of 5FU by infusion with CPT-11 was shown to be associated with reduced toxicity and an apparent improvement in survival as compared to that of administration of the drug by bolus injection with CPT-11.[1,2] This synergistic enhancement may result from the mechanism of action of the 2 drugs; CPT-11 has been reported to cause accumulation of cells in the S phase, and 5FU infusion is known to cause DNA damage specifically in cells of the S phase.[14] On the basis of this background, our results suggesting the more pronounced and more prolonged accumulation of the tumor cells in the S phase caused by NK012 as compared with that by CPT-11 may explain the more effective synergy of the former administered with 5FU infusion. This may be attributable to accumulation of NK012 due to the enhanced permeability and retention (EPR) effect.[9] It is also speculated that NK012 allows sustained release of free SN-38, which may move more freely in the tumor interstitium.[15] Otherwise NK012 itself could internalize into cells to localize in several cytoplasmic organelles as reported by Savic *et al.*[16] These characteristics of NK012 may be responsible for its more potent antitumor activity observed in this study, because CPT-11 has been reported to show time-dependent growth-inhibitory activity against the tumor cells.[17]

The major dose-limiting toxicities of CPT-11 are diarrhea and neutropenia. SN-38, the active metabolite of CPT-11, may cause CPT-11-related diarrhea as a result of mitotic -inhibitory activity.[18] Because it undergoes significant biliary excretion, SN-38 may have a potentially long residence time in the gastrointestinal tract that may be associated with prolonged diarrhea.[19,20] In our previous report, we evaluated the tissue distribution of SN-38 after administration of an equimolar amount of NK012 (20 mg/kg) and CPT-11 (30 mg/kg), and found no difference in the level of SN-38 accumulation in the small intestine.[12] A significant antitumor effect of NK012 with a lower incidence of diarrhea was also dem-

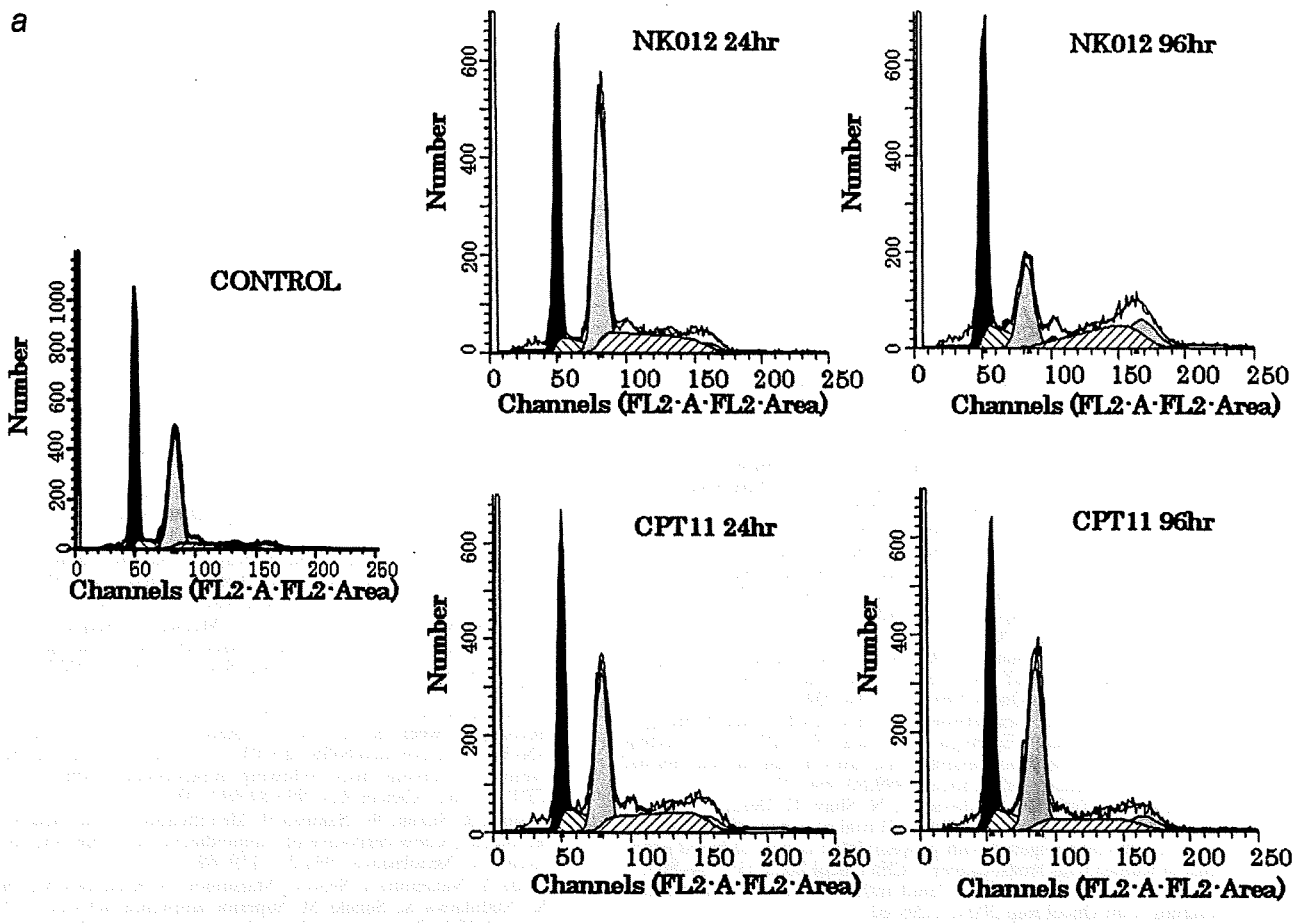

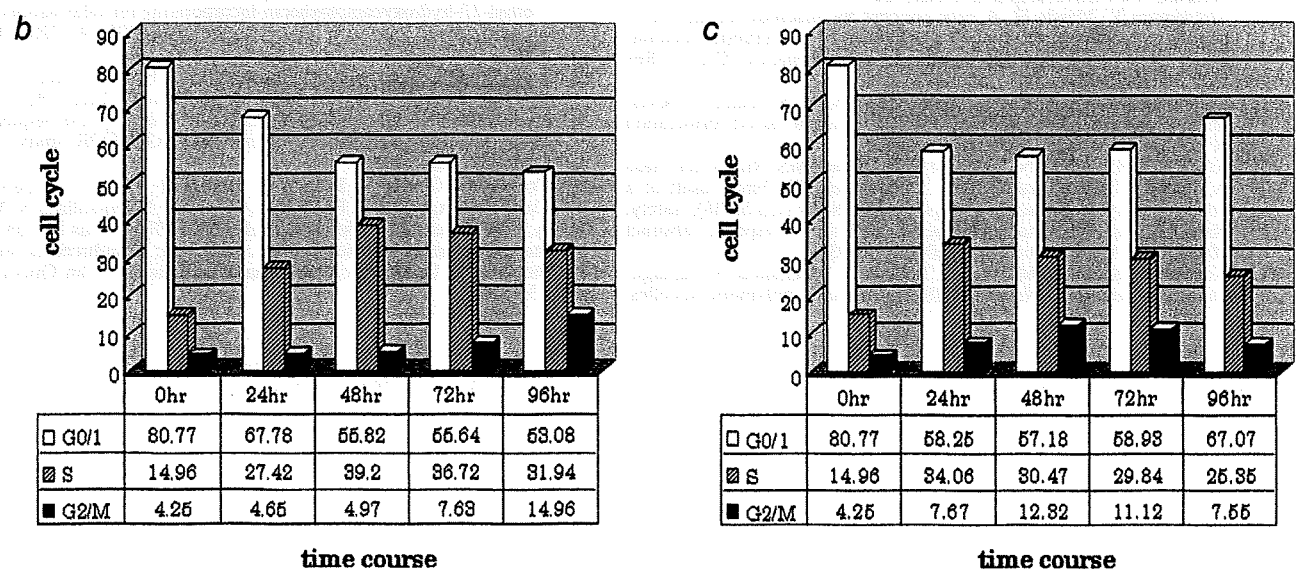

	0hr	24hr	48hr	72hr	96hr
□ G0/1	80.77	67.78	55.82	55.64	53.08
▨ S	14.96	27.42	39.2	36.72	31.94
■ G2/M	4.25	4.65	4.97	7.63	14.96

	0hr	24hr	48hr	72hr	96hr
□ G0/1	80.77	58.25	57.18	58.93	67.07
▨ S	14.96	34.06	30.47	29.84	25.35
■ G2/M	4.25	7.67	12.32	11.12	7.55

FIGURE 4 – Cell cycle analysis of HT-29 tumor cells collected 24, 48, 72 and 96 hr after administration of NK012 at 10 mg/kg alone or CPT-11 at 50 mg/kg alone using the Modfit program (Verity Software House Topsham, ME). (*a*) Cell cycle analysis of HT-29 tumor cells 24 and 96 hr after administration of NK012 at 10 mg/kg or CPT-11 at 50 mg/kg, respectively. (*b*) Cell cycle distribution of tumor cells 0, 24, 48, 72 and 96 hr after treatment with NK012 at 10 mg/kg. (*c*) Cell cycle distribution of tumor cells 0, 24, 48, 72 and 96 hr after treatment with CPT-11 at 50 mg/kg.

onstrated as compared to that observed with CPT-11 in a rat mammary tumor model.[21] Combined administration of CPT-11 with 5FU/LV infusion appears to be associated with acceptable toxicity in patients with CRC. In addition, no significant difference in the frequency of Grade 3/4 diarrhea was noted between patients treated with FOLFIRI (CPT-11 regimen with bolus and infusional 5FU/LV) and those treated with FOLFOX6 (oxaliplatin regimen with bolus and infusional 5FU/LV).[22,23] Our *in vivo* data actually revealed no severe body weight loss in the NK012/5FU group. Consequently, we expect that the NK012/5FU regimen, especially